Quantitative differential Proteomics for Analysis of Posttranslational Modifications of Proteins

Dissertation zur Erlangung des Grades

Doktor der Naturwissenschaften

Am Fachbereich Biologie

der Johannes Gutenberg-Universität Mainz

MSc Slobodan Poznanović

geboren in Belgrad, Jugoslawien

Mainz, 2008

Summary

In this work we developed a new and convenient method for high resolution IEF of proteins, which we termed: "daisy chain". Usually an IEF is accomplished with IPG strips of a desired pH range. For high resolution focusing we are using strips with pH range, which covers only one or two pH units. Thereby the proteins, which have isoelectrical point outside of this pH range, are lost. We evaluated commercially available IPG strips with consecutive or overlapping pH ranges and connected them serially acidic to basic end, to construct in this way a high resolution IEF-system. For the first time, we showed that a high resolution IEF is possible in such a system and that results were by no means worse than those obtained when the same sample was analyzed on individual single IPGs. The great advantage of our system is that amount of sample used in serial IPG IEF is explicitly lower than when same sample was analyzed on individual single IPGs. This method was subsequently successfully applied to valuable clinical samples from cancer patients and to mitochondrial preparations related to a European project in gerontology. We thus developed a suite of experimental strategies, which adequately address complex biological situations, in particular on the level of protein expression.

Im Rahmen dieser Arbeit wurde eine neue und effiziente Methode zur hochauflösenden Isoelektrischen Fokussierung (IEF) von Proteinen entwickelt, die wir "daisy chain" nennen. Üblicherweise wird eine Fokussierung in IPG-Streifen mit einem gewünschten pH-Bereich durchgeführt. Für hochauflösende Fokussierungen werden Streifen verwendet, in denen der pH-Bereich nur ein oder zwei pH-Einheiten umfasst. Dabei gehen die Proteine, die einen isoelektrischen Punkt ausserhalb dieses pH-Bereichs sitzen verloren. Um diesen Probenverlust zu verhindern, untersuchten wir in Serie verbundene kommerziell erhältliche IPG-Streifen mit genau aufeinanderfolgenden oder überlappenden pH-Bereichen. Es wurde zum ersten Mal gezeigt, dass eine hochauflösende Fokussierung mit seriell verbundenen IPG-Streifen möglich ist. Die Ergebnisse waren gleichwertig mit Fokussierungen in einzelnen IGP-Streifen, aber mit dem Vorteil des deutlich reduzierten Probenbedarfs. Diese Methode wurde anschließend erfolgreich zur differenziellen protemischen Analyse von wertvollen klinischen Tumorproben sowie von mitochondrialen Extrakten im Rahmen eines EU-geförderten Gerontologie-Projektes eingesetzt. In Verbindung mit dieser neuen, hochauflösenden IEF wurden experimentelle Strategien entwickelt, mit denen Fragestellungen bezüglich der Proteinexpression in komplexen biologischen Systemen adequat addressiert werden können.

mojim roditeljima

List of abbreviations

µA	Microampere
µCi	Microcurie
µg	Microgram
µL	Microliter
16-BAC	Benzyldimethyl-n-hexadecylammonium Chlorid
2D-PAGE	Two-dimensional polyacrylamide gel electrophoresis
AA	Acrylamide
APS	Ammonium Persulfate
ATP	Adenosine triphosphate
BCA	Bicinchoninic acid
BPB	Bromophenol blue
BSA	Bovine serum albumine
CAPS	N-cyclohexyl-3-aminopropanesulfonic acid
CBB	Coomassie Brilliant Blue
cDNA	complementary Deoxyribonucleic acid
CHAPS	3-[(3-Cholamidopropyl)dimethylammonio]-1-propanesulfonate
cm	Centimetre
CO_2	Carbon dioxide
CRABP-II	cellular retinoic acid binding protein type II
Cy3	Indocarbocyanin 3
Cy5	Indocarbocyanin 5
DIGE	differential in-gel electrophoresis
DNA	Deoxyribonucleic acid
DTT	Dithiothreitol
e.g.	exempli gratia
EDTA	Ethylendiamin-N,N,N´,N´-tetraacetic acid
ER+	estrogen receptor positive
ESI	Electrospray ionization
FCS	Fetal Calf Serum
Fe_2SO_4	Ferrous sulphate
g	Gram
GRAVY	General average hydropathicity
H	Hour
H_2O_2	Hydrogen peroxide
HCl	hydrochloric acid
I	Iodine
ICAT	isotope-coded affinity tagging
IDPm	NADP+-dependent isocitrate dehydrogenase
IEF	Isoelectric focusing
IPG	Immobilized pH gradients
K_3PO_4	Tribasic potassium phosphate
kBq	Kilobecquerel
kDa	kilodalton
LC	Liquid chromatography
LCM	Laser capture microdissection
LMPC	Laser microdisection and pressure catapulting
M	Molar concentration
MΩ	Megaohm
MALDI TOF	Matrix-assisted laser desorption/ionization time of flight

MBq	Megabecquerel
MDA	malondialdehyde
min	Minute
mL	Milliliter
mm	Millimeter
mM	Millimolar
MOPS	3-(N-morpholino)propanesulfonic acid
MPTP	mitochondrial permeability transition pore
mRNA	Messenger ribonucleic acid
MS	Mass spectrometry
mtDNA	Mitochondrial DNA
MudPIT	multidimensional protein identification technologies
MW	Molecular weight
$Na_2S_2O_3$	Sodium thiosulfate
NADP	Nicotinamide adenine dinucleotide phosphate
NADPH	Nicotinamide adenine dinucleotide phosphate (reduced form)
NaOH	Sodium hydroxide
ng	nannogram
NO	nitric oxide
pH	potentia hydrogenii
pI	Isoelectric point
PMF	peptide mass fingerprinting
PR+	progesterone receptor positive
RCC	renal cell carcinoma
RNA	Ribonucleic acid
ROS	reactive oxygen species
RT	room temperature
SDS	sodium dodecyl sulfate
SELDI	surface enhanced laser desorption ionization
TBP	Tributylphosphine
TCA	Trichloroacetic acid
TEMED	Tetramethylethylenediamine
TFA	Trifluoroactetic acid
TPCK	L-1-tosylamido-2-phenylethyl chloromethyl ketone
Tris	Tris-(hydroxmethyl)-aminomethan
UV	Ultraviolett
V	Volt
Vh	Volthours
W	Watt
WHO	World Health Organization
x g	times gravity (units of gravity)

Index of Figures

Index of Tables

Table of Contents

1 Introduction

The term "proteome" was first introduced by Wilkins and Williams to indicate the entire "PROTEin" complement expressed by a "genOME" of a cell, tissue, or entire organism (Wilkins et al., 1996). The intrinsic flexibility of the genome is only unfolded on the level of highly dynamic proteomes dependent upon the ontogenetic, and thus epigenetic situation of an individual organism at a given point in time. It changes with the state of tissue development or under influence of environmental and nutritional conditions and is characterized by an enormous molecular complexity. The number of posttranslational protein isoforms is typically many millions multiplied from genomes consisting of a much smaller number of genes (e.g. approx. human 20,000 genes (Stein, 2004)). On the way from a gene to an mRNA-transcript, alternative splicing and RNA-editing are mechanisms that provide already a considerable degree of inflation of numbers of molecules. Additionally, and most importantly there exist hundreds of chemical posttranslational modifications causing manifold modular adaptation of the same amino acid backbone of a given protein. Due to this huge variety of alterations one of the famous dogmas of biology, the one-gene-one-protein hypothesis (Beadle and Tatum, 1941) is no longer tenable without a certain degree of relativity.

Proteome analysis or "proteomics" has been growing rapidly since its introduction. It should be noted that proteomics has gradually replaced or complemented "functional genomics", at the same time heavily depending on methods and data base tools developed during the "genomic" era. Large-scale nucleic acid–based studies, employing e.g. cDNA microarrays, have been shown to provide much more indirect but nevertheless related biological information. Thus, the increasing integration of proteomics, transcriptomics and genomics data in the sense of a truly "systems biology" approach, has recently attracted considerable attention (Butcher, 2005).

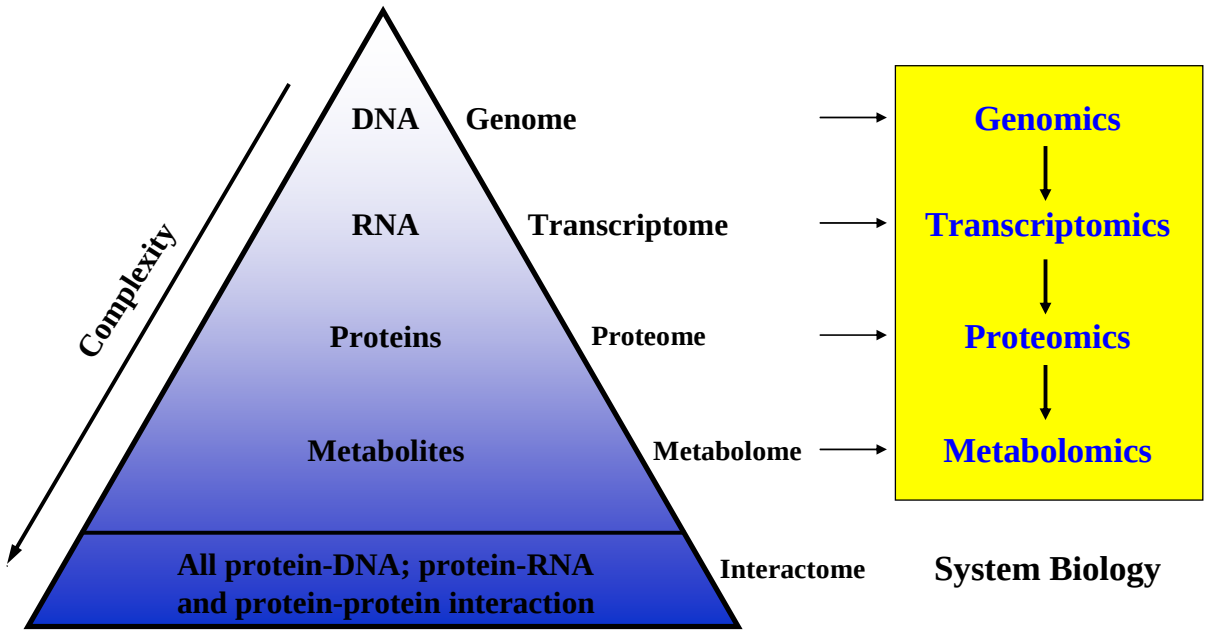

Figure 1: Definition of -omics

Today, the scope of proteomics is continuously increasing, comprising not only mapping efforts concerning expression of proteins in certain tissues, and all types of biological or clinical samples, but also protein interactions with other molecules at a variety of conditions and with an increasing focus on relatively fast kinetics of posttranslational modifications. Therefore proteomics can be defined as the core discipline of the emerging field of systems biology (Figure 1)

1.1 Separation – Resolution – Differential quantification

Modern proteomics is confronted with two major problems:

- Dynamic expression range (protein abundance) (Corthals et al., 2000)
- Diversity of protein expression (multiple protein forms) (Harry et al., 2000)

The problem of dynamic expression range is especially dramatic in body fluids like plasma. Some abundant proteins e.g. albumins and immunoglobulins are present in much higher concentrations than other proteins, obscuring the detection of less abundant proteins. Removing high abundant proteins from complex mixtures is considered to facilitate the detection of low abundant ones. Depending upon concentrations of low abundant proteins and available amounts of sample, very often situations are encountered when is not possible at all to detect

proteins of interest beyond e.g. highly abundant serum albumin. For every experiment novel compromises concerning resolution and dynamic range of detection have to found (Schrattenholz and Groebe, 2007). 2D-PAGE, although the method with the high resolution is limited by dynamic ranges of detection methods (Table 1).

Number of cells	Protein copies/cell	Protein molecules	Moles of protein	50 kDa Protein (ng)	Visualization limit
10^9	100000	10^{14}	160 pmole	8300	Coomasie blue
10^9	1000	10^{12}	1.6 pmole	83	Silver stain
10^9	10	10^{10}	16 fmole	0.80	Radioactive
10^6	100000	10^{11}	160 fmole	8	Silver stain
10^6	1000	10^9	1.6 fmole	0.08	Radioactive
10^6	10	10^7	16 amole	$8x10^{-5}$	No detection

Table 1: Detection limit of proteins in mixture calculated on 100% recovery basis

Since many of the low abundant (low number of protein copies per cell) proteins have important regulatory functions in cells, it is clear that the separation of low abundant proteins in amounts sufficient for subsequent mass spectrometry-based identification is one important issue in proteome studies and one of the major present analytical challenges. This problem can be partially overcome either by increasing separation power or involving prefractionation steps to enrich low abundance proteins (Washburn et al., 2001). So, the stochasticity and complexity of protein expression is the most considerable conceptual challenge of molecular biology and medicine (Schrattenholz and Soskic, 2006) next to reliable methods for rigid differential quantitative pattern control, (Schrattenholz and Groebe, 2007) in systems biology and Proteomics, novel statistical and mathematical strategies are required for the interpretation of any given protein expression profile at any given point in time.

Proteomics is specially suited for drug discovery because drug modes of action mostly affect proteins. Thus protein surrogate biomarkers defining differences between various stages of treatments increasingly generate effort and interest (Marko-Varga et al., 2005; Rajasethupathy et al., 2005; Duncan and Hunsucker, 2005) and fuel the development of a wide array of separation technologies, ranging from 2D-PAGE (Huang et al., 2006), mass spectrometry-linked liquid chromatography (Fujii et al., 2004), capillary electrophoresis (Servais et al.,

2006) or chip-based SELDI (Wright, Jr., 2002). These powerful methods currently generate enormous amounts of data and the necessity of data management and quantitative interpretation presents one of the most pressing needs of molecular medicine.

A Biomarker can be defined as a molecule, which indicates an alteration of the physiological state of an individual organism in relation with healthy and diseased functional states. It can be influenced by drug treatment, toxins and others changes in the environment. Potential biomarkers need to be validated in large-scale studies involving bigger numbers of cases and independent detection methods (e.g. antibodies). The chemical diversity of proteins is underlying the necessity of improved resolution of applied technologies to obtain quantitative information which otherwise could be lost in pools of poorly resolved peptides.

1.2 Sample complexity defines application of proteomics technologies

Biomarkers and indeed protein isoforms carry important functional information about disease stages and are used clinically to diagnose or to monitor progression or remission. They are used as guide to molecular targeted therapy or to access therapeutic response (Etzioni et al., 2003). Modern clinical diagnostics urgently needs better biomarkers to improve diagnosis and that is exactly place where modern proteomics can contribute most.

Modern proteomics is an umbrella for a wide variety of experimental technologies (Schrattenholz and Groebe, 2007; Mann, 2006; Forner et al., 2006; Gingras et al., 2007; Schmidt and Aebersold, 2006; Ong and Mann, 2007). Until mid 1990, proteins were mostly characterized by amino acids sequencing with Edman degradation technique (Edman and Begg, 1967). This method, although very powerful for characterization of individual proteins, is relatively complicated and not very well suited for analysis of complex protein mixtures. With introduction of 2D PAGE followed with in-gel digestion of protein spots and subsequent analysis of peptide mixture with mass spectrometry, we approach real analysis of complex protein mixture (Henzel et al., 1993; Shevchenko et al., 1996).

Two-dimensional gel-electrophoresis (2D PAGE) coupled with mass spectrometry-based protein identification is the classical tool of proteomic analysis. The capability of 2D-PAGE to separate thousands of proteins in a single analysis

and to make a direct comparison of proteins expressed in various functional conditions made it the method of choice for the search of new biomarkers and disease-related profiling of protein expression (Issaq and Veenstra, 2007). 2D-PAGE has been described as labor intensive, low performance and a technique that requires high amounts of sample. Notwithstanding, 2D-PAGE today is still preferred for large-scale separation of complex protein mixtures. Main advantage in comparison with other techniques is resolution – it is actually still the best alternative due to high-resolution separation in first dimension isoelectric focusing and second dimension SDS-PAGE. However there are limitations as well: some hydrophobic membrane proteins or structural proteins or very basic and very acidic proteins do not easily enter IEF gels. Another limitation of 2D PAGE is the reproducibility of the usually quite complex patterns in independent experiments, which requires rigorous and laborious pattern control strategies described below. On the other side, next to improved resolution, the very fact of ever-independent experiments instead of memory-effects of e.g. LC columns might represent a trade-off for limited throughput.

Key for success of 2D PAGE-based biomarker discovery is a detection method enabling differential quantification. Three possibilities exist: radioactive and stable isotope labelling and fluorescent dyes. Stable isotope labelling can be directly coupled to mass spectrometry (MS): methods range from surface enhanced laser desorption and ionization (SELDI), isotope-coded affinity tagging (ICAT) to multidimensional protein identification technologies (MudPIT) and imaging mass spectrometry.

Further separation technologies used in proteomics include multidimensional liquid chromatography (LC), capillary electrophoresis, protein arrays, various fractionation techniques, including immunoaffinity depletion and other affinity-based approaches.

1.3 Cancer Proteomics

Among complex diseases, there is strong genetic component in many types of cancer. Moreover, on a functional level, cancer is characterized by chromosomal aberrations and epigenetic phenomena, which are essentially caused by the pressure of the immune system, which cancer cells need to avoid. During carcinogenesis, genetic defects are selected only in case if they provide a survival

advantage for cancer cells (Hanahan and Weinberg, 2000). These defects lead to tumor cell survival by altering functional protein expression, protein networks and signaling pathways (Liotta and Kohn, 2001). The completion of sequencing the human genome (Stein, 2004), and the resulting enormous amounts of data, has contributed much less than anticipated to a better understanding of complex diseases like a cancer.

And so, modern societies continue to pay a very high price in terms of death and quality of life caused by various forms of cancer. The hope of fast and easy cures has not been fulfilled, but the genomic information available has provided proteomics with the sequence-based framework for investigation of cancer-related proteomes. In particular the search of new surrogate biomarkers for early diagnosis as well as for discovering of new therapeutics for a wide range of conditions has gained considerable steam by the application of quantitative and differential exploration of well characterized clinical samples by appropriate proteomics technologies, which are chosen according to the sample complexity and biological necessity (Schrattenholz and Groebe, 2007). Today biomarkers top the list of activities for early diagnosis of cancer and drug discovery. There are two main approaches:

- Large scale analysis of gene expression at the RNA level (Reis et al., 2005)
- Use of various proteomic methods.

The potential of 2D-PAGE in analysis of cancer has been demonstrated a long time ago by examination of 14 lung tumors (Okuzawa et al., 1994). There were variations in the expression of several proteins, which correlate with different histological types as well as specific over expression of one particular protein. Similar approaches have been applied to breast cancer (Wirth et al., 1987; Rasmussen et al., 1997) and kidney tumors (Sarto et al., 1997).

They are two main forms of using 2D-PAGE in cancer research. The first and conventional one is comparing expression level of proteins in two samples – one normal and one pathological by generating several 2D replicas for each sample. At the end this method generates two master 2D gels – one from normal and one from pathological sample which are then used for analysis of up or down regulation of particular proteins.

Comparing several different gels can always lead to systematic error because matching of independent experiments is a non-trivial problem. This problem can be avoided by running two samples in one experiment or more precisely using one gel. This is a second form of using 2D in cancer research and is termed differential display. Currently there are three methods for this type of proteomic differential display:

- DIGE (differential in-gel electrophoresis) – from Amersham Bioscience (GE Health care today) using fluorescent cyanine dyes Cy3 and Cy5 (Unlu et al., 1997).
- ProteoTope –labeling with radioactive isotopes (Wozny et al., 2007).
- ICAT (isotope coded affinity tag) from Applied Biosystems, that uses labeling with stable isotopes.

2D-PAGE in combination with mass spectrometry (MALDI and Electro spray) represents a very powerful tool in cancer proteomics. The in depth clarification of specific posttranslational modifications of proteins in tumor tissue can be restricted by the simple fact of insufficient amounts of isolate of specific cell type from pathological samples. Given the huge dynamic range of protein concentrations and the discussion of low abundance proteins above, the tumor microenvironment consists not only of e.g. malignant epithelial components but as well as of stroma and normal tissue. Over the years many different strategies have been used to optimize sample preparation. Cell scrapping and affinity column separation (Franzen et al., 1995), and manual microdissection of tissue sample (Radford et al., 1993) are some of them. All these methods actually suffer from contamination and the inability to remove specific subpopulations of cancer cells. As soon as laser capture microdissection was introduced (Emmert-Buck et al., 1996), the way for the isolation of specific subpopulations of cancer cells was opened. For laser capture microdissection a transparent thermoplastic film (vinyl acetate polymer) is applied onto the surface of a tissue section previously immobilized on glass. With help of CO_2 laser pulses, surface above the cell of interest can be activated and removed. Cell subpopulations of interest can thus be isolated from rest of the tissue, representing a much focused type of biological fractionation. PALM micro systems, inc., have modified this method in so far that tissue is mobilized directly into collecting devices.

The aim was the isolation of very specific populations of cancer cells is thus brought to analysis, digging directly into cancer metabolism. This work has contributed to the application of laser capture microdissection in proteomics.

2 Material and Methods

2.1 Chemicals and Reagents

All chemicals and reagents used in this work were pro analysis quality and were obtained from different companies listed in table below. Special attention has been paid to water quality. For casting of IEF gels, it has been found that MilliQ water using a Millipore device (>18 MΩ) is exceptionally important.

List of used chemicals

α-cyano-4-hydroxycinnamic acid	Sigma, Taufkirchen
6-Aminocaproic acid	Sigma, Taufkirchen
Acetic acid	Roth, Karlsruhe
Acetonitrile,	Riedel-de Haen, Seelze
Acrylamide p.a.	Amersham Biosciences
Acrylamide solution 30%	Roth, Karlsruhe
Agarose, ultra pure	BioRad, Hercules (USA)
Ammonium persulfate (APS)	Sigma, Taufkirchen
Ascorbic acid	Sigma, Taufkirchen
BCA – protein determination kit	Pierce, Rockford (USA)
Benzyldimethyl-n-hexadecylammonium Chlorid (16-BAC)	Sigma, Taufkirchen
Bis-Tris	Sigma, Taufkirchen
Bromophenol blue	Sigma, Taufkirchen
CAPS	Sigma, Taufkirchen
CHAPS	Gerbu, Gaiberg
Citric acid	Fluka, Buchs (CH)
Coomassie Brilliant Blue G250	Serva, Heidelberg
Coomassie Brilliant Blue R250	Serva, Heidelberg
Deoxycholic Acid Sodium Salt	Sigma, Taufkirchen
Dithiothreitol (DTT)	Calbiochem, Darmstadt
EDTA	Sigma, Taufkirchen
Ethanol absolut	Roth, Karlsruhe
Ethylenediamine	Sigma, Taufkirchen
Ferrous Sulfate heptahydrate	Fluka, Buchs (CH)
Fetal Calf Serum (FCS)	Gibco, Karlsruhe
Formaldehyde, p. a.	Sigma, Taufkirchen
Glutaraldehyde	Fluka, Buchs (CH)
Glycerol	Roth, Karlsruhe
Glycine	Sigma, Taufkirchen
Hydrochloric acid p.a.	Merck, Darmstadt
Immobiline	Amersham Biosciences
Iodacetamide	Sigma, Taufkirchen
IPG buffer (different pH)	Amersham Biosciences
IPG strips (different pH range)	Amersham Biosciences
Methanol	Riedel-de Haen, Seelze
MOPS	Sigma, Taufkirchen
n-Dodecyl β-D-maltoside	Fluka, Buchs (CH)
Pefablock SC	Merck, Darmstadt
Phosphoric acid 85% p.a.	Merck, Darmstadt

Potassium bromide	Sigma, Taufkirchen
Potassium phosphate dibasic	Sigma, Taufkirchen
Potassium phosphate monobasic	Sigma, Taufkirchen
Pre-Coated Iodination tubes	Pierce, Rockford (USA)
Protease inhibitor cocktail CompleteTM (PIC)	Boehringer, Mannheim
Servalyt pH 6-9	Serva, Heidelberg
Silver nitrate	Sigma, Taufkirchen
Sodium acetate p.a.	Sigma, Taufkirchen
Sodium carbonate p.a.	Sigma, Taufkirchen
Sodium dodecylsulfate (SDS)	Sigma, Taufkirchen
Sodium hydroxide	Merck, Darmstadt
Sodium phosphate dibasic	Sigma, Taufkirchen
Sodium phosphate monobasic	Sigma, Taufkirchen
Sodium thiosulfate pentasulfate	Fluka, Buchs (CH)
β-4-Hydroxyphenyl-ethyl-iodacetamid	Pierce, Rockford (USA)
TEMED	Sigma, Taufkirchen
Thiourea ulta pure	Fluka, Buchs (CH)
Tributylphosphine (TBP)	Fluka, Buchs (CH)
Trichloroacetic acid (TCA)	Sigma, Taufkirchen
Tricine	Sigma, Taufkirchen
Trifluoroactetic acid (TFA)	Fluka, Buchs (CH)
Tris	Sigma, Taufkirchen
Tris-HCl	Sigma, Taufkirchen
Triton X-100	BioRad, Hercules (USA)
Tween 20	BioRad, Hercules (USA)
Urea p.a.	Fluka, Buchs (CH)

2.2 Instrumentation and Equipment

List of used instruments

Electrophoresis

Ettan DALT II system	Amersham Biosciences
HCN 140–35000 Power supply unit	F.u.G. Elektronik, Rosenheim
Hoefer DALT system	Amersham Biosciences
Hoefer SE 600	Amersham Biosciences
IPGphor	Amersham Biosciences
Protean IEF cell	Bio-Rad, Hercules (USA)
Scanner FLA 3000	Fuji Film, Düsseldorf
Scanner Umax PowerLook II	Umax Systems, Willich
Slab Gel Dryer	Savant
Speed Vac	Savant

Mass spectrometry

MALDI Ultraflex TOF/TOF	Bruker-Daltonics, Bremen
ESI-Ion trap Esquire 4000	Bruker-Daltonics, Bremen
ProPick robot	Genomics solutions Ltd, Huntington
ProGest robot	Genomics solutions Ltd, Huntington

Miscellaneous

Centrifuge Biofuge Fresco	Heraeus, Langenselbold
Centrifuge Biofuge Prima R	Heraeus, Langenselbold
Centrifuge Sigma 3K30	Sigma, Osterode am Harz
Laboratory pipettes Reference	Eppendorf, Hamburg
Spectrophotometer Sunrise	Tecan, Crailsheim
Thermomixer comfort	Eppendorf, Hamburg

2.3 Isoelectric focusing (IEF)

2.3.1 High resolution IEF gels: "Daisy chain" setup

2.3.1.1 Casting of "bridges" for IEF-"Daisy chain"-gels

During the course of this work, a novel high resolution 2D-PAGE method has been developed and successfully introduced to cancer proteomics (Poznanovic et al., 2005a). In detail, the mold, consisting of two glass plates, one covered with the Gel Bond PAG film, the other with a U-frame (0.5 mm thick), is loaded in a vertical position and filled from the top. Prior to use, glass plates are thoroughly washed with a mild detergent, rinsed with MilliQ water and air-dried. If new glass plates are used, 1-2 mL of repellent silane is pipetted onto the glass plate using the U-frame and distributed evenly with a lint-free paper (Kimwipe). After drying for a few minutes, plates were rinsed again with water and air-dried again. This procedure was repeated in order to prevent gels from sticking to the glass plates.

Gel Bond PAG films were washed 3 x 10 min with MilliQ water prior to use. Gels must be casted onto the treated, hydrophilic side of Gel Bond PAG film (film is packed with the treated side up with paper interleaving to protect the treated surface). Prior to assembly of the polymerisation cassette, the plain glass plates (size 260 x 200 mm) were wetted with a few drops of water. Gel Bond PAG film was placed, hydrophilic side upwards, on the wetted surface of the plain glass plate. The Gel Bond PAG film should overlap the upper edge of the glass plate for 1-2 mm to facilitate filling of the cassette. Surface of Gel Bond PAG film was covered with Kimwipe paper and excess of water was expelled with a roller (Figure 2).

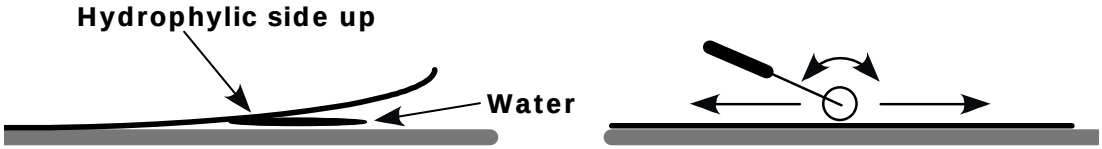

Figure 2: Assembling glass plate with Gel Bond PAG film

For casting bridges, a 4% acrylamide (AA) solution was prepared. Mold was filled with 20 mL of AA solution and left 15 min at room temperature (RT). Final polymerization of the gel was performed for 1 hour at 50 °C. After polymerization at 50 ° C, the gels were allowed to cool down to RT for at least 15 min. Mold was disassembled by inserting spatula between gel and glass plate. Support film with gel was carefully removed and washed 4 x 15 min with MilliQ water. Finally, gels were incubated in 2% glycerol for 30 min. Gels were dried overnight in a hood or with a fan (for several hours). Dried gels were covered with Gel cover film (Serva) and cut into 3.5 mm wide stripes.

2.3.1.2 Rehydration of gels

IEF Buffer

(7 M urea, 1% Triton-X-100, 10% glycerol, 2M thiourea, 4% CHAPS, 20 mM Tris pH 7.4, 1% DTT)

Urea	5.255 g
Triton-X-100	0.125 g
Glycerol	1.25 g (1mL)
Thiourea	1.9 g
CHAPS	0.5 g
Tris pH 7.4	
1.5 M Tris pH 7.4	166 µL
DTT	0.125 g
MilliQ H_2O	Ad 12.5 mL

1% Bromophenol blue-Solution (500x)

Final concentration: 0.002% ≈ 0.028 mM; 20 mg Bromophenol blue in 2 mL MilliQ-H_2O

For high-resolution "daisy" chain gels, commercial IPG strips from Amersham Biosciences were used. Strips were rehydrated according to manufacturer's instructions. Depending on appropriate sample application strategies, the following scheme was generally used:

pH of IPG strip	Case A (in-gel Rehydration)	Case B (wick application)
4-5	Sample + IEF buffer with 0.8% of IPG buffer pH 3.5-5.0	IEF buffer with 0.8 % of IPG buffer pH 3.5-5.0
5-6	IEF buffer with 0.8 % of IPG buffer pH 5.0-6.0	IEF buffer with 0.8 % of IPG buffer pH 5.0-6.0
6-9	IEF buffer with 0.8 % of Serva-lyt CA pH 6.0-9.0	IEF buffer with 0.8 % of Serva-lyt CA pH 6.0-9.0
Bridges	IEF buffer with 0.8% mix of IPG buffers 3.5-5.0; 5.0-6.0 and Servalyt 6.0-9.0 1:1:1	IEF buffer with 0.8% mix of IPG buffers 3.5-5.0; 5.0-6.0 and Servalyt 6.0-9.0 1:1:1

Table 2: IPG buffer scheme for indicated pH-ranges

Usually "in gel" rehydration method was used. 350 µg of protein in IEF buffer (Table 2) were mixed with IEF buffer and IPG buffer to give final volume of 340 µL.

2.3.1.3 Assembling of high resolution "daisy chain"-gels

Rehydrated IPG strips were blotted with wet Whatmann paper and daisy chain gels were assembled either in 100 cm or 65 cm trays. Before assembly, laminated grid paper was placed under the trays for alignment of the IPG strips. The tray was filled with paraffin oil prior to assembling of strips. Plastic ends of the IPG strips were cut before alignments according to following scheme:

- IPG strip pH 4-5: Plastic end was cut at cathodic ("-" or basic) end
- IPG strip pH 5-6: Plastic ends were cut both at anodic ("+" or acidic) and cathodic ("-" or basic) end
- IPG strip pH 6-9: Plastic end was cut at anodic ("+" or acidic) end

If several daisy chain gels were to be assembled, the best way to do this was to align first IPG strips pH 4-5, than IPG strips pH 5-6 by attaching acidic part of the IPG strip to the basic end of IPG strip pH 4-5 and finally IPG strips pH 6-9 by attaching acidic part of the IPG strip to the basic end of IPG strip pH 5-6. After all IPG strips were in the tray, final alignments were done (Figure 3).

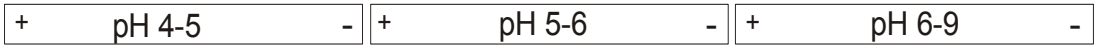

Figure 3: Alignments of IPG strips in Daisy chain

After aligning all IPG strips, paper wicks with loaded sample were assembled. Electrode-paper wicks (3 cm wide and long enough to cover all IPG strips) were placed over IPG strips on both acidic and basic end of a daisy chain gel.

Finally, electrodes were assembled. In case of wick application, the electrode-paper wick for the anode (+) was soaked in 10 mM orthophosphoric acid, and the one for the cathode (-) was soaked in MilliQ water. In another case, when samples were applied by in-gel rehydration, both (+) and (-) electrode-paper wicks were soaked in MilliQ water. Bridges (AA strips rehydrated in buffer as described above) were treated in the same way as any IPG strip. After blotting on wet paper they were cut into approx. 1 cm long pieces. Bridges were taken carefully with forceps and positioned down "gel on gel" over ends of two IPG strips.

2.3.1.4 IEF run condition for "daisy chain"-gels

Typical running condition:

150 V for 30 min
300 V for 30 min
600 V for 30 min
3000 V up to 10000 Vh
10000 V up to 100000 Vh
1000 V up to 24 h
Current is limited to 50 µA per strip

After focusing, IPG strips were immediately equilibrated (see below) and second dimension PAGE was started. In the case, that second dimension PAGE could not be run immediately; IPG strips were shortly blotted to remove oil and stored at –20°C until further use.

2.4 Second-dimension: SDS PAGE

2.4.1 Casting vertical 12 % SDS PAGE

2.4.1.1 Buffers and solutions

To run 2D SDS PAGE following buffers and solutions were prepared:

1.5 M Tris / HCl pH 8.8

181.68 g Tris base
800 mL MilliQ H_2O
pH adjusted with conc. HCl
ad 1000 mL MilliQ H_2O

Equilibration buffer

50 mM Tris/HCl pH 8.8; 6M urea; 30% glycerol; 2% SDS

20 mL 0.5 M Tris/HCl pH 8.8
72 g urea
60 mL glycerol
4 g SDS
ad 200 mL MilliQ H_2O

Equilibration buffer I

Equilibration buffer with 1% DTT

10 mL equilibration buffer
100 mg DTT

Equilibration buffer II

Equilibration buffer with 4.5% iodoacetamide

10 mL equilibration buffer
450 mg iodoacetamide

10x Electrophoresis running buffer

60.6 g Tris base
288 g glycine
20 g SDS
ad 2000 mL MilliQ H_2O

10% SDS solution

10 g SDS
ad 100 mL MilliQ H_2O

Displacing solution

50 mL 1.5 M Tris/HCl pH 8.8
100 mL 99% glycerol
40 µL 2.5% BPB in 50% ethanol
ad 200 mL MilliQ H_2O

0.5% Agarose solution

0.25 g agarose
5 mL 10x Electrophoresis buffer
10 µL 2.5% BPB in 50% ethanol
45 mL MilliQ H_2O

30% Acrylamide, 0.8% Bis-Acrylamide

Ready solution from Carl Roth; Catalogue 3029.1

10% Ammonium persulfate

500 mg APS
ad 5 mL MilliQ H_2O

2.4.1.2 Casting of gels

Gels for second dimension were casted in a Hoefer DALT Multiple Gel Caster. The DALT gel caster can accommodate twenty-five 1 mm gel cassettes. Original glass cassettes (25.5 x 20.4 cm) were used. Slab gel size was 1.00 mm x 23.4 x 19.5 cm. Prior to the setup of the gel caster, glass plates cassettes were washed with ethanol and wiped with lint-free paper. The DALT gel caster was filled with glass cassettes and setup performed according to the instruction manual. Before pouring of gel solution through funnel, the balance chamber was loaded with 150 mL of heavy displacing solution. The following recipe was used to prepare 1500 mL of 12% acrylamide gel solution:

30% AA; 0.8% Bis-AA	600 mL
1.5 M Tris/HCl pH 8.8	375 mL
MilliQ H_2O	505 mL
At this point, the gel solution was degassed for 15 min with vacuum pump	
10% SDS	15 mL
10% APS	4.3 mL
TEMED	300 µL

The solution was poured slowly to avoid forming of air bubbles. Once pouring was complete, the feeding tube from the balance chamber grommet was removed to allow the heavy displacing solution to flow down. The displacing solution pushes the remaining acrylamide solution into the gel cassettes. Finally, cassettes were overlaid with water-saturated n-butanol. Gels were allowed to polymerize 2 hours at RT. After disassembling of the gel caster, gels were used immediately or stored at +4 ºC until further use.

2.4.2 Running 2D SDS PAGE

IPG strip equilibration

Equilibration of strips was always performed prior to second dimension run. Strips were equilibrated in two steps in equilibration buffers I and II. After finishing IEF, rest of paraffin oil was shortly blotted; strips placed in a tray for equilibration (Bio-Rad) and covered with a few milliliters of equilibration buffer I containing DTT. Equilibration was performed at RT for 15 min with shaking. Strips were than transferred to another tray and covered with equilibration buffer II containing Iodoacetamide. Like in first step, strips were equilibrated for 15 min with shaking. This equilibration step is important to reduce point streaking and

other artifacts. In the case when IEF wasn't done prior to second dimension, frozen strips were shortly (several minutes) defrosted at RT and equilibration was done as described above.

Applying the equilibrated IPG strip

Previously casted second dimension gels were drained from rest of storage buffer and positioned in the rack. Molecular weight marker protein solution was applied on a paper wick and with forceps dipped on a left side (marked as "+" or acidic side position for IPG strip) of the gel. Previously equilibrated IPG strips were dipped shortly in electrophoresis buffer (to lubricate strips) and pushed down completely, between two glass plates, so that entire lower edge of an IPG strip was in contact with top surface of the slab gel. It is necessary to ensure that no air bubbles are trapped between IPG strip and slab gel surface. Finally, strip was sealed down with 0.5% of agarose solution. After several minutes (necessary agarose to gel) plates were positioned in electrophoresis chamber, previously filled with 18 liters of electrophoresis running buffer. Additional amount of electrophoresis running buffer was added if necessary and electrophoresis was started.

Electrophoresis condition

Typical electrophoresis was run overnight with buffer cooled to 20 °C, under following conditions: Constant 80V for 18-22 h, subsequently voltage was raised to 200V until BPB reached the front.

2.4.3 Silver staining of gels

Buffers and solutions

Fixing solution

50% ethanol, 12% acetic acid

	1 L
Ethanol	500 mL
Acetic acid	120 mL
MilliQ H_2O	380 mL

0.02% Sodium thiouslfate

	1 L
Sodium thiosulfate	0.314g
MilliQ H20	1000 mL

0.1 % (w/v) Silver nitrate solution

	1 L
Silver nitrate	1 g
MilliQ H20	1000 mL

Developer

2% (w/v) Sodium carbonate, 0.0185% formaldehyde

	1 L
Sodium carbonate	30 g
MilliQ H20	1000 mL
Formaldehyde (37% Solution)	0.5 mL

Stop solution

2% Acetic acid/4% Tris base

	1 L
Acetic acid	20 mL
Tris base	40 g
MilliQ H20	ad. 1000 mL

Procedure

Fixation of gels after electrophoresis:	1 x 45 min
Washing of gel in MilliQ H_2O:	3 x 20 min
Incubation in 0.02% Na2S2O3:	1 x 1 min
Washing of gel in MilliQ H_2O:	2 x 30 sec
Incubation in 0.1 % Silver nitrate:	1 x 30 min
Washing with MilliQ H_2O:	2 x 1 min
Washing with developer:	1 x 10 sec
Developing of gels:	Incubation in developing solution with light shaking until sufficient color developed. The development should be stopped when the background starts to become too dark.
Stopping of developing:	1 x 15 min

Scanning of gels

After staining, gels were scanned with UMAX PowerLook II scanner at 16 bit grey scale with a resolution of 200 dpi. The resulting pictures were saved as tiff format files.

2.5 1D SDS PAGE

We run several different 1D SDS PAGE gels. They were prepared according to standard procedures and here only necessary buffers and solutions are listed. Further details will be discussed in text below.

2.5.1 Blue Native SDS PAGE

2.5.1.1 Buffers and solutions

First dimension cathode buffer

50 mM Tricine, 15 mM Bis-Tris, 0.02% CBB G-250, pH 7.0
8.95 g Tricine 15 mL 1M Bis-Tris pH 7 0.2g CBB G-250 ad 1000 mL MilliQ H_2O

First dimension anode buffer

50 mM Bis-Tris pH 7.0
50 mL 1M Bis-Tris pH 7.0 ad 1000 mL MilliQ H_2O

Blue native extraction buffer

500 mM 6-aminocaproic acid, 100 mM Bis-Tris pH 7.0, 1% laurylmaltoside, Protease inhibitors
6.56 g 6-aminocaproic ac. 10 mL 1M Bis-Tris pH 7.0 1g laurylmaltoside 2 complete Protease inhibitor tablets ad 100 mL MilliQ H_2O

Equilibration solution

50 mM Tris pH 6.8, 4% SDS, 50 mM DTT, 30% glycerol
1 mL 0.5M Tris pH 6.8 0.4 g SDS 100 µL 5M DTT in H_2O 3 g glycerol ad 10 mL MilliQ H_2O

2.5.2 16-BAC SDS PAGE

2.5.2.1 Buffers and solutions

16-BAC Sample buffer

2.25 g Urea 0.5 g 16-BAC 0.5 mL glycerol 4 mL H_2O heat at 60 °C to dissolve 0.75 mL 1.5 M DTT 50 µL of 5% pyronine Y ad 10 mL MilliQ H_2O

Equilibration solution

50 mM Tris pH 6.8, 4% SDS, 50 mM DTT, 30% glycerol
1 mL 0.5M Tris pH 6.8
0.4 g SDS
100 µL 5M DTT in H_2O
3 g glycerol
ad 10 mL MilliQ H_2O

Ferrous sulfate

5 mM solution (prepare prior to use)
13.9 mg Fe_2SO_4x7 H_2O
ad 10 mL MilliQ H_2O

Ascorbic acid

80 mM ascorbic acid (prepare prior to use)
140.9 mg ascorbic acid
ad 10 mL MilliQ H_2O

Electrode buffer (10x)

2.5 mM 16-BAC, 150 mM glycine, 50 mM phosphoric acid
1,0 g 16-BAC
11,26 g glycine
2,9 mL phosphoric acid (85%)
ad 1000 mL MilliQ H_2O

Fixing solution

Isopropanol:acetic acid:water=3.5:1:5.5
350 mL isopropanol
100 mL acetic acid
550 mL MilliQ H_2O

2.5.2.2 Recipe of 16-BAC gel for 1st dimension

7.5% Separation gel (40 mL)

Urea	7.2 g
30% AA; 0.8% Bis-AA	10 mL
300 mM K_3PO_4, pH 2.1	10 mL
1.7 % Bis-acrylamide	1.4 mL
80 mM Ascorbic acid	2 mL
5 mM Fe_2SO_4	64 µL
250 mM 16-BAC	400 µL
MilliQ H_2O	10 mL
30 % H_2O_2 (1:600 diluted)	500 µL
Polymerization (2 h)	

4% Stacking gel (10 mL)

Urea	1 g
30% AA; 0.8% Bis-AA	1.33 mL
500 mM K_3PO_4, pH 4.1	2.5 mL
1.7 % Bis-acrylamide	1.38 mL
80 mM ascorbic acid	500 µL
5 mM Fe_2SO_4	8.5 µL
250 mM 16-BAC	70 µL
MilliQ H_2O	3 mL
30 % H_2O_2 (1:1200 diluted)	200 µL
Polymerization (overnight)	

2.5.3 Tricine / Urea SDS PAGE

2.5.3.1 Buffers and solutions

Tricine / Urea Sample buffer

50 mM Tris pH 6.8, 2% SDS, 10% glycerol, 50 mM DTT, 0.02% Coomassie G 250

2 mL 10% SDS
1 g glycerol
100 µL 5 M DTT
1 mL 0.5 M Tris pH 6.8
ad 10 mL MilliQ H_2O

Cathode buffer (10x stock)

0.1 M Tris, 0.1 M Tricine, 0.1% SDS

121 g Tris
179.2 g glycine
10 g SDS
ad 1000 mL MilliQ H_2O

Anode buffer (10x stock)

0.2 M Tris-HCl pH 8.9

242 g Tris
Adjust pH with HCl
ad 1000 mL MilliQ H_2O

2.5.3.2 Recipe of Tricine/Urea-Tricine gel for 1st dimension

10% Separation gel

Urea	14.4 g
30% AA; 0.8% Bis-AA	13.32 mL
4M Tris-HCl, pH 8.45	9.99 mL
10 % SDS	400 µL
Glycerol	4 mL
MilliQ H_2O	ad 40 mL
10% APS	200 µL
Temed	12 µL

4% Stacking gel

Urea	3.6 g
30% AA; 0.8% Bis-AA	1.33 mL
4M Tris-HCl, pH 8.45	1.88 mL
10 % SDS	100 µL
MilliQ H_2O	ad 10 mL
10% APS	50 µL
Temed	3 µL

2.5.3.3 Recipe of Tricine/Urea-Tricine gel for 2nd dimension

16.5% Separation gel

30% AA; 0.8% Bis-AA	22 mL
4M Tris-HCl, pH 8.45	10 mL
10 % SDS	400 µL
Glycerol	4 mL
MilliQ H_2O	ad 40 mL
10% APS	200 µL
Temed	12 µL

4% Stacking gel

30% AA; 0.8% Bis-AA	1.33 mL
4M Tris-HCl, pH 8.45	1.88 mL
10 % SDS	100 µL
MilliQ H_2O	ad 10 mL
10% APS	50 µL
Temed	3 µL

2.6 Renal Cell Carcinoma proteomics

2.6.1 Preparation of histological sections and LMPC

Tissue samples were obtained from the Department of Urology at Maximilian University in Munich with written permission from a 72-year-old female patient after surgery of kidney tumor. Immediately after surgery, blocks of tumor and surrounding normal kidney tissue were excised, frozen in liquid nitrogen and stored at -80 °C until further use. Frozen tissue blocks were cut with Cryostat (Leica) into 10 µm thick sections. Sections were transferred to PALM Membrane Slides (P.A.L.M. Microlaser Technologies AG, Bernried, Germany), air-dried for 1 min on ice and then fixed for 2 min in pre-cooled (-20 °C) 75% ethanol. An experienced pathologist had examined and classified the tumor as RCC of the clear-cell type, T3bN0M0G (Storkel et al., 1997).

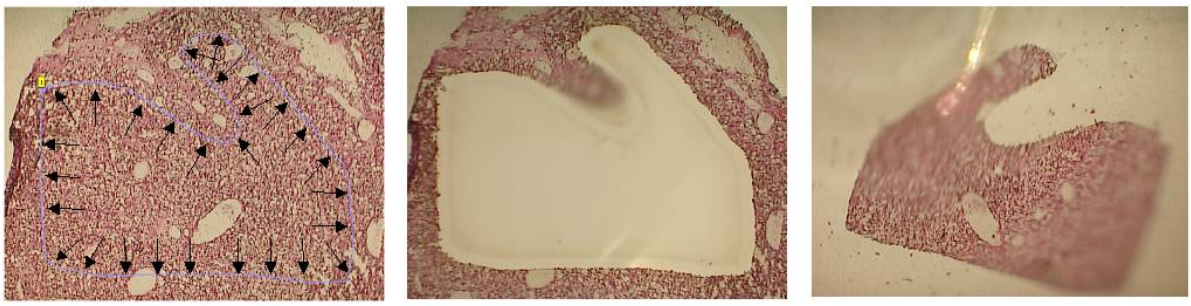

Figure 4: LMPC of cancer tissue A) Blue line show selected tumor area to be excised by LMPC. B) Tissue with excised tumor cells. C) Excised tumor cells in collection buffer

Laser microdisection and pressure catapulting technology was used to obtain high uniformity of samples tissue areas of tumor (cancer) and nontumor (normal) areas (total amount 7.5 mm^2). For collection the 337 nm UV-laser based PALM MicroBeam system (P.A.L.M. Microlaser Technologies AG, Bernried, Germany) was used. Selected cell areas were cut with a pulsed UV-laser beam controlled by the PALM RoboSoftware around the desired area and then catapulted into a collection device (Figure 4). For protein analysis the cap of a 500 µL microfuge tube was filled with 20 µL of 8M urea, 4% CHAPS, in 0.1M Tris, pH 7.4, for sample collection. Samples were frozen and stored at –80 °C. Samples for tracer gels were obtained by collecting 30 cryoslices of 10 µm thickness from kidney tumors or healthy tissue respectively. Collected cryoslices were solubilized in 200 µL of 8M urea, 4% CHAPS, 0.1M Tris pH 7.4, frozen and stored at -80 °C.

2.6.2 ProteoTope

2.6.2.1 Iodination of samples

For analytical ProteoTope 2D gels, LMPC dissected samples in 8 M urea, 4% CHAPS, 0.1 M Tris pH 7.4 were thawed at 25 °C, and samples were than incubated at room temperature for 30 min with shaking in a Thermo mixer comfort (Eppendorf). Finally samples were centrifuged for 5 min at 20,000 x g and RT. Supernatants were removed and sample volume was adjusted to 20 µL. Each micro dissected sample was aliquoted into two identical 10 µL aliquots and pipetted into pre-coated Iodogen tube (Pierce). Approximately 6 MBq of $Na^{125}I$ or $Na^{131}I$ (circa 162 µCi), respectively, were added to Iodogen tubes, and the final volume was set to 25 µL. Samples were incubated for 20 minutes at RT and further proceed as described (Vuong et al., 2000).

Prior to cold iodination with non-radioactive iodine, samples for tracer gel analysis were thawed, incubated at RT and centrifuged as described above. Protein concentration was determined using the BCA method (Pierce). From cancer tissue we obtained 795 µg of protein and from normal tissue 1135 µg of protein. Proteins were iodinated with non-radioactive NaI using same the Iodogen method as for radio-labeling.

2.6.2.2 2D-PAGE

After Iodination we determined incorporation of iodine into proteins, and 90 kBq of ^{125}I and 90 kBq of ^{131}I (approximately 2.4 µCi, presenting 8-10% of labeling reaction yield) were applied in 100 µL IEF buffer onto a 1x5x15 mm paper wick. 2D-PAGE was performed using 18 cm commercial IPGs in serial 54 cm IPG-IEF "daisy chain" over pH 4-9 (pH 4-5; pH 5-6; pH 6-9) as described here (Poznanovic et al., 2005a). Paper wick with radio labeled proteins was placed between the electrode and the pH 4-5 IPG at the anodic side of IEF gel. Running conditions for isoelectric focusing were as described above.

For tracer gel analysis 240 µg of cold-iodinated proteins were loaded by in-gel rehydration to pH 4-5 IPG strip of daisy chain serial IPGs. Trace of ^{125}I-labeled protein from either normal or tumor samples (90 kBq) used for analytical ProteoTope analysis (see above) was loaded by anodic wick loading similarly as described above and coelectrophoresed with coldly iodinated sample. Analytical and tracer IEF gels were run in 2D SDS-PAGE as 3 x 18 cm IPGs in a Hoefer ISO-

DALT system. Tracer IEF gels were run in the second dimension SDS-PAGE on gels that were polymerized onto glass plates using Bind-Silane (Sigma) and silver stained as described in this work.

2.6.2.3 Gel imaging

Spot detection and quantification was performed using the PIC/GREG software (Fraunhofer-Institut für Angewandte Informationtechnik, Sankt Augustin), using parameters optimized for ProteoTope images as described (Schrattenholz et al., 2005). Spots were chosen as differential when abundance ratio was at least 2-fold, and statistical probability was less than 0.05. Synthetic average images for presentation were made with Delta2D (Decodon GmbH, Greifswald, Germany) (Schrattenholz et al., 2005).

2.6.2.4 Scanning of the gels

The silver stained (tracer) gels were dried, optically scanned, and then exposed to radioactive measurement by ProteoTope. Radioactive ProteoTope tracer gel images were aligned by computer-based gel matching with GREG software to the corresponding images of the same samples from differential microdissected sample gel images.

2.6.2.5 Mass spectrometry

Silver stained spots that were comigrating with selected radioactive spots were cut out with ProPick robot from the rehydrated silver-stained preparative gel, digested with TPCK trypsin in ProGest robot and subjected to MALDI-TOF peptide mass fingerprinting (Vogt et al., 2003).

2.7 Breast Cancer proteomics

2.7.1 Patients and tissue samples

Primary breast cancer specimens were obtained from patients, at the Department of Gynecology and Obstetrics, University Hospital Tübingen with permission from patient and ethical commission of the medical faculty. Samples were characterized and collected by an experienced pathologist. After surgical removal of breast tumor from the patient, the tissue samples were embedded in a special low-temperature embedding medium for cryosectioning (OCT from Leica), then frozen in liquid nitrogen within 15 minutes of tumor removal, and

stored in liquid nitrogen in a tumor tissue bank. An experienced pathologist had established histopathological diagnosis according to the current WHO classification of breast tumors, and resulting data were stored in the Path-Report-database of the Institute for Pathology (Tübingen). Later this data base was used to select cryopreserved tumor samples. For this work we selected 24 tumors from a total of 250 tumors. Selected tumor samples were re-diagnosed and quality of tumor tissue was verified by measuring RNA integrity from one or more slices with an Agilent 2001 Bioanalyzer. Tumors missing 18S and 28S ribosomal RNA bands were excluded from the study. Collected samples with clinical and pathological information as well with clinical data for each patient are summarized in Table 3.

Experimental variable designation	Pools	Tumor number	LCM shots	RNA quality	Tumor status	Grade	ER status	PR status	Her2/neu-status	Age of patient	Preparative slices	Preparative pooled yield
ER+/PR+	PR + 1	T 698	10000	OK	pT2	2	12	12	0	65	35	4313 µg
		T 851	10000	OK	pT1	2	12	9	0	78	35	
		T 876	10000	OK	pT2	2	12	9	0	70	35	
	PR + 2	T 259	10000	OK	pT1	2	12	9	0	70	35	
		T 533	10000	OK	pT2	2	12	12	1	65	35	
		T 630	10000	OK	pT1	2	12	12	0	70	35	
	PR + 3	T 415	10000	OK	pT2	2	12	8	0	67	35	
		T 595	10000	OK	pT2	2	12	8	0	73	35	
		T 764	10000	OK	pT2	2	12	12	0	42	35	
	PR + 4	T 794	10000	OK	pT1	2	12	12	1	65	35	
		T 816	10000	OK	pT1	2	12	6	0	66	35	
		T 869	10000	OK	pT1	2	12	12	0	64	35	
ER+/PR-	PR - 1	H 623	10000	OK	pT2	2	12	0	0	56	35	3390 µg
		H 69	10000	OK	pT2	2	12	0	0	59	35	
		T 680	10000	OK	pT2	2	12	0	2	38	35	
	PR - 2	H 579	10000	OK	pT1	2	12	0	0	63	45	
		T 382	10000	OK	pT1	2	12	0	0	57	55	
		T 894 I	10000	OK	pT1	2	12	0	0	65	45	
	PR - 3	T 425 III	10000	OK	pT2	2	12	0	0	78	45	
		T 413	10000	OK	pT3	2	12	0	1	60	35	
		T 802	10000	OK	pT2	2-3	12	0	0	76	35	
	PR - 4	H 574 II	10000	OK	pT2	2	12	0	0	76	55	
		T 2	10000	OK	pT2	2	12	0	1	77	35	
		T 228	10000	OK	pT3	2	12	0	0	62	45	

Table 3: Samples with histological parameters used in this work and distribution of sample pools

2.7.2 Preparation of histological sections, LMCP and sample pooling

Selected tumor samples from the cryo tissue database, were removed from the cryo tissue bank on dry ice, transferred to a cryotome (Leica) at a temperature of -25°C and cut into 10 µm tick sections. These were placed on Super-Frost+ slides (Multimed) and further stored at -80°C until LMPC. For selection of tumor cells suitable for laser microdissection, one section was stained with hematoxilin/eosin.

Tumor cells were isolated using a laser capture microscope Arcturus PixCell IIe supplied with 355 nM UV laser. We acquired 10,000 LCM shots from each tumor samples, using a pulsed 30 µm laser-focus setting. Approximately seven cells were harvested with each laser pulse (total of 70000 cells). Cells were stored at -80°C until further use. Samples from three separate LCM harvested ER+/PR- or ER+/PR+ tumors were pooled giving in total 30000 LCM shot equivalents per pool. From this pool, 10,000 shot equivalents were used for labeling with ^{125}I, 10,000 shot equivalents were labeled with ^{131}I, and 10,000 shot equivalents were used to make a pool of all 12 patients for each condition (Table 3). The joint pools of all 12 patients for each condition were iodinated with ^{125}I and used as radioactive tracer in preparative gels.

2.7.3 ProteoTope

Samples for ProteoTope analysis (Schrattenholz et al., 2005) were prepared more or less as described above. We didn't alkylate cysteines prior to iodination. Microdissected samples in LCM caps were solubilized in 8 M urea, 4% CHAPS, 0.1M Tris pH 7.4 at 25°C, and samples were than incubated at RT for 30 min with shaking in Thermomixer comfort (Eppendorf). Finally samples were centrifuged for 5 min at 20,000 x g and RT. Supernatants were removed, samples volume was adjusted to 20 µL and aliquots were taken to construct pooled samples of three tumours per pool (Table 3). Aliquots of these pools (approximately 3.6 µg pooled sample) were pipetted into pre-coated Iodogen tube (Pierce). Approximately 6 MBq of $Na^{125}I$ or $Na^{131}I$ (circa 162 µCi), respectively, were added to Iodogen tubes, and final volume was set up to 25 µL. Samples were incubated for 20 minutes at RT and further processed as described (Vuong et al., 2000). A joint pool of 12 patients for each ER/PR condition was iodinated with ^{125}I.

2.7.3.1 2D PAGE and Gel Imaging

2D-PAGE was performed essentially as described above for renal cell carcinoma, using 18 cm commercial immobilized pH gradients (IPGs) in serial 54 cm IPG-IEF over pH 4-9 (pH 4-5; pH 5-6; pH 6-9) that were run in the SDS-PAGE dimension as 3 x 18 cm IPGs in a Hoefer ISO-DALT.

2.8 Mitochondrial proteome

2.8.1 Preparation of mitochondria from bovine heart

Mitochondria were isolated from bovine heart obtained at a local slaughter-house from a freshly killed animal. Half of the heart muscle was processed shortly after slaughtering and the rest was cut in small cubes, frozen in liquid nitrogen, and stored at –80 °C until further use. Heart muscle was homogenized, mitochondria were prepared by differential centrifugation using ice-cold buffers as described (Smith, 1967). Obtained mitochondria were resuspended in 250 mM sucrose, 10 mM Tris-HCl, 1 mM Tris-succinate pH 7.8, 0.2 mM EDTA, 0.5 mM Pefabloc SC and frozen in liquid nitrogen. Material was aliquoted in 500 µL fractions and stored at -80 °C for a maximum of 6 month after the day of preparation.

2.8.2 16-BAC SDS PAGE

100 µL aliquot of mitochondria membrane suspension (about 1470 µg of proteins) was resuspended in 1500 µL of 8M Urea + PIC and sample was further incubated for 30 min at RT. The sample was divided in two half's, 800 µL each and centrifuged at 20,000xg for 30 minutes. One of the obtained pellets was dissolved in 100 µL of 16-BAC sample buffer (see above) and incubated 5 min while shaking. 50 µL of sample dissolved in 16-BAC sample buffer was applied on 7.5% 16-BAC gel and run 45 min at 100 V and 4 h at 350 V. The gel was fixed overnight in 3.5:1:5.5 isopropanol : acetic acid : water and stained with Coomassie R-250. For second dimension SDS PAGE, gel lines were excised and strips were incubated 5 min at +95 °C in 4% SDS, 30% glycerol, 50 mM DTT, 50 mM Tris pH 6.8 at +95 °C. Lanes were layered on top of the gel and covered with 0.6% agarose in running buffer. Electrophoresis was performed overnight in Hoefer SE 600 gel electrophoresis system. Gels were finally stained with silver nitrate.

2.8.3 Tricine-Urea/Tricine SDS PAGE

Tricine-urea/Tricine electrophoresis were performed as described (Schagger and von Jagow, 1987) with modifications described in (Rais et al., 2004). 28 µL aliquot of mitochondria membrane suspension was resuspended in 150 µL of sample buffer and incubated for 30 minutes at RT while shaking. Sample was centrifuged at 20,000xg and 50 µL (about 100 µg of protein) were applied on top

of 10% acrylamide 6M Tricine/urea gel. Electrophoresis were performed overnight in Hoeffer SE 600 chamber with cooling at 15 C and 70 V. For the 2nd dimension two lanes were excised and incubated for 5 minutes in 4% SDS, 30% glycerol, 50 mM DTT, 50 mM Tris pH 6.8 at +95 C. Gel pieces with protein lanes were placed on top of 16.5% Tricine gel in Hoeffer SE 600 chamber. Electrophoresis were performed overnight at constant 70V with cooling at + 15 °C. The gels were stained with Coomassie R-250 or silver nitrate as describe before.

2.8.4 Blue Native SDS PAGE

Blue-native PAGE was performed using the Hoefer SE 600 system (18×16 cm) as described previously (Schagger, 2001). To separate stable oxidative phosphorylation complexes, a slight modification as described (Krause et al., 2005) was applied (Schagger and Pfeiffer, 2000; Krause et al., 2004). A previously prepared mitochondrial membrane suspension (20 µL) was resuspended in 150 µL of blue native extraction buffer (500 mM 6-aminocaproic acid, 100 mM bis-Tris pH 7.0, 1% laurylmaltoside, and PIC tablet) and incubated 60 minutes on ice. The sample was further mixed with 20 µL glycerol and 10 µL of 5% Coomassie G-250 in 500 mM 6-aminocaproic acid and incubated 10 minutes. An aliquot of 50 µL was loaded directly on top of 5-13% blue-native gradient gel overlaid with 3% stacking gel. Electrophoresis was run with cooling at +4 °C at 100 V until the samples completely entered separating gel. Voltage was than limited to 500 V, 15 mA and gel was running until dye front reach gel bottom (4-5 hours). Blue native gel lanes were excised from gel and incubated for 5 minutes at +95 C in 4% SDS, 50 mM DTT, 30% glycerol, 50mM Tris pH 6.8. Gel lanes were subsequently loaded on 13% Tricine SDS-PAGE second dimension gel with 5% stacking gel and run overnight at constant 80 V. Gels were stained with Coomassie R-250 and Silver nitrate.

2.8.5 2D PAGE “Daisy chain”

An 100 µL aliquot of mitochondrial membrane suspension (about 1470 µg of proteins) was dissolved in 1500 µL of 8M Urea + PIC and the sample was further incubated for 30 min at RT while shaking in a Thermomixer comfort. The sample was divided in two half’s a 800 µL each and centrifuged at 20,000xg for 30 minutes. One of the pellets was dissolved in 100 µL of 2% SDS, 50 mM Tris pH 7.4 and incubated 5 min at +95 °C. The protein solution was applied on Pierce Protein desalting column previously equilibrated in IEF sample buffer. 300 µg of pro-

tein were loaded for the overnight rehydration to the pH 5-6 IPG strip. IPG strips pH 4-5 and pH 6-9 were rehydrated in IEF sample buffer with corresponding IPG buffer. After overnight rehydration IPG strips were run in serial IEF "daisy chain" and second dimension was performed as described above and elsewhere (Poznanovic et al., 2005a).

2.8.6 Protein identification

Gel image analysis of the silver stained gels was performed with Pic/Greg software (Fraunhofer-Institut für Angewandte Informationtechnik, Sankt Augustin). The main criteria to select protein spots for picking were spot volume (at least 1.e10 units used by Greg software) and background intensity (at least four times less than spot intensity). The final decision, which spots to process, was met after manual inspection using the Pic program, in this way avoiding artifacts.

Selected spots were excised from the gel by a ProPick picking robot and gel pieces were digested with TPCK trypsin using a ProGest-robot. Digested samples were subjected to MALDI-TOF peptide mass fingerprinting (Vogt et al., 2003). Mass spectra of peptide ions were obtained using an Ultraflex MALDI TOF mass spectrometer and the resulting peptide mass fingerprints were searched against an NCBI Protein Sequence Database using Mascot Server software v. 1.8. (Matrix Science, London, UK) (Cahill et al., 2003; Sommer et al., 2004).

3 Results

3.1 Technical solution: Serial IPG gels – "Daisy Chain" gels

Before completion of this work, the production of long IPG gels (Poland et al., 2003) required specialized equipment and know-how. An appropriate commercial system for gel casting was not available on the market during development of long IPG gels.

Therefore, the aim of this work was whether the system could be simplified using commercially available IPGs. The main idea was to connect ends (acidic to basic) of commercially available IPGs to construct in this way a high resolution IEF-system tantamount to previously developed continuous long gels, which however suffered from poor reproducibility.

3.1.1 Equipment for running of "Daisy chain" gels

Again, running of IEF with long IPG gels was not possible without special equipment. On the market there didn't exist anything commercially available. Thus, it was necessary to develop own equipment to meet the special demands of high resolution IEF with ultra-long IPG's (54 cm).

3.1.1.1 IPG strip tray

Isoelectric focusing with IPG strips is possible without using paraffin oil. In this case, there is a very high risk of urea crystallizing on the gel surface, due to electroendoosmosis. Although electroendoosmosis exists even when IPG strips are covered with oil during IEF, the risk of crystallizing urea is explicitly smaller (Westermeier et al., 1983). In order to run IEF under oil, a tray with glass bottom dimensions of 940 mm x 145 mm was constructed, with 18 mm high walls. The tray may be compared to an oversized standard tray from Immobiline dry strip kit from Amersham Bioscience.

3.1.1.2 Cooling device

First experiments with "daisy chain" gels were run without additional cooling. For the sake of reproducibility between experiments, uniform running conditions are a must, and since temperature is one of the major parameters influencing electrophoretic mobility, a cooling device was constructed. The first model

was made from glass. Temperature was controlled by circulation of temperated water. The results weren't completely satisfactory because glass was conducting temperature quite poorly, and thus fine control of temperature wasn't possible. Moreover, the whole device was very heavy and fragile. For better results we consequently developed an aluminum cooling device, similar to the one in Amersham Bioscience Multiphor II system (dimensions 1100 mm x 240 mm). This cooling device was connected to an Amersham Bioscience MultiTemp Thermostatic circulator.

3.1.1.3 Electrodes

Electrodes were made from Plexiglas using 1 mm thick platinum wire of high quality obtained from Degussa Austria. To fulfill the German safety regulations for voltages above 10,000 V (VDE 0411), electrodes and cable were prepared by Wagner Elektroanlagenbau (Nackenheim; Germany) according to our instructions.

3.1.1.4 IEF chamber

The IEF chamber developed during the course of this work consists of:

- Water-cooled aluminum device
- IPG strip tray placed onto this device, with oil between the glass and metal surfaces to facilitate thermal transfer. IPGs were placed onto the bottom surface of this tray.
- To insulate against high voltage during IEF entire assembly was placed in a closed Plexiglas chamber.

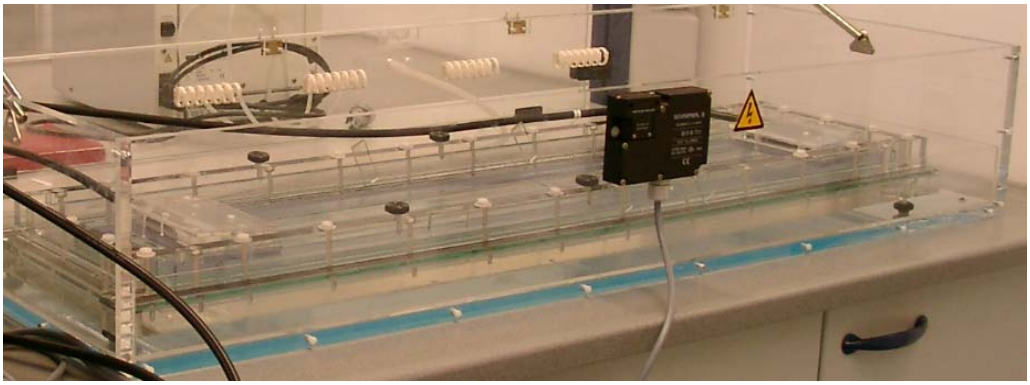

Figure 5: IEF chamber

The assembled device might be functionally described as an oversized Pharmacia MultiPhor IEF chamber. The hinged lid was fitted with a delayed safety catch to prevent opening until voltage in the power supply had subsided to safe levels (Figure 5).

3.1.1.5 Power supply

The power supply unit was an HCN 140–35,000 (F.u.G. Elektronic, Rosenheim Germany), programmable from 0-35,000 V at 0–4 mA in 50 µA steps. An in-house computer program controlled the unit. This device was internally custom-modified to accommodate the above lid-opening safety delay circuitry by Wagner Elektroanlagenbau (Nackenheim, Germany), who also provided all cables, electrical connections and self-made electrodes according to our instructions and German safety regulations for voltages above 10,000 V (VDE 0411).

3.1.1.6 Assembling of Daisy chain

To avoid problems with CO_2, isoelectric focusing was performed in the presence of several pieces of 3MM paper (30 x 300 mm) soaked in 1 M NaOH. Papers were distributed in the chamber adjacent to the IPGs. Additionally, prior to the start of IEF, the chamber was saturated with argon.

3.1.2 Bridging

It was found that proteins could migrate through connecting bridging material from one IPG to another during IEF in serial IPG "daisy chains" with surprisingly high efficiency (Figure 6). We tested agarose, various types of paper and polyacrylamide gels as bridging material. Although high-grade agarose may sometimes be suitable, 3MM paper and polyacrylamide bridges gave superior results. Eventually, the best results were obtained by using polyacrylamide gel bridges, which became routine in our laboratory.

It was interesting to investigate whether IPGs could themselves serve as chain bridges. In the experiment shown in Figure 7 no particular bridges were used. Middle IPG pH 5-6 was inverted (plastic baking film up and gel surface down) and serves as the bridge between the IPGs pH 4-5 and pH 6-9. We found that no obvious deterioration in the quality of results using this experimental design. I note, however, that with this design, no uniform cooling of the IPG pH 5–

6 was secured. The risk of damage to this IPG if incorrectly handled is high. Therefore, the use of acrylamide bridges was preferred in the end, despite the risk that some proteins may be retained in these bridges.

3.1.3 Carrier ampholytes

To find out best condition for IEF run it was tested a variety of combinations of different sources of commercially available carrier ampholytes. None of these combinations, however, were superior to those supplied by the manufacturer in the recommended concentration for each IPG.

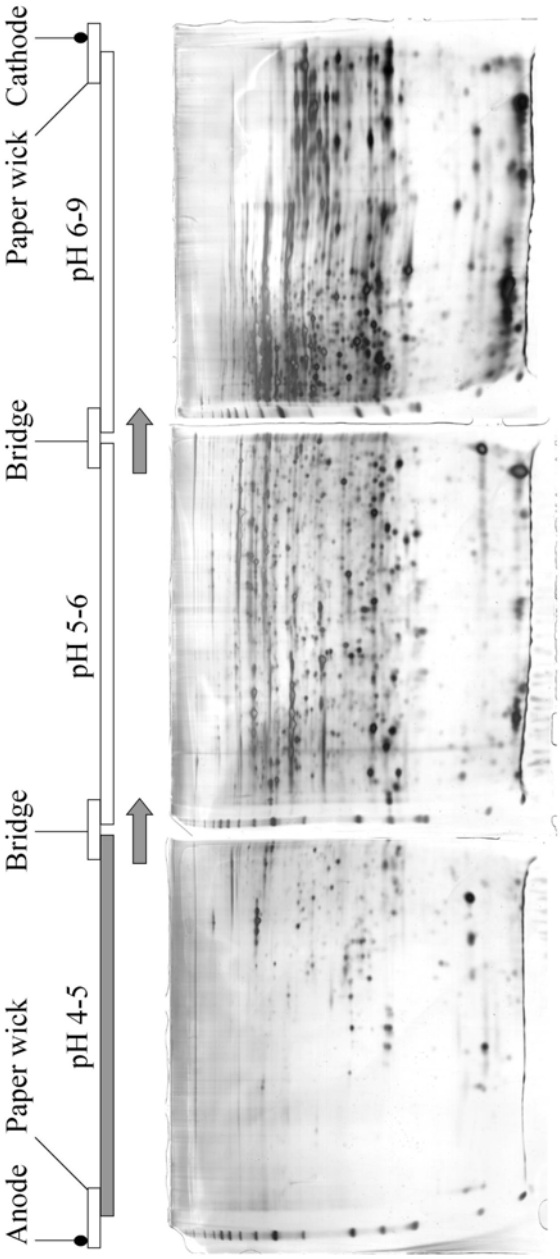

Figure 6: Example of a serial IPG experiment (top), with corresponding 2-D PAGE gels for each IPG below the diagram.

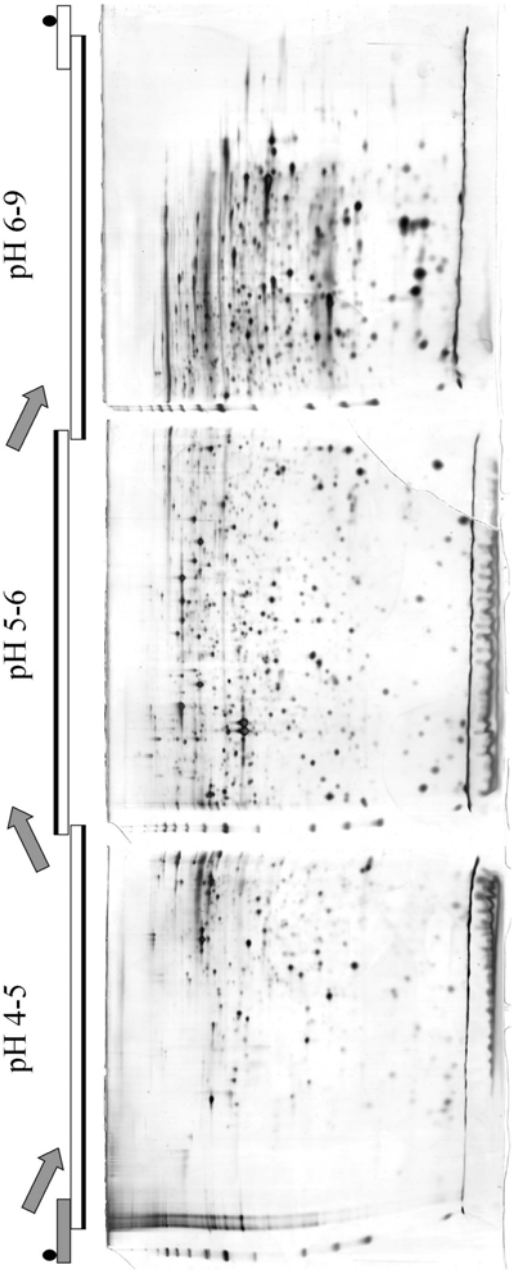

Figure 7: A schematized example of daisy chain experiment where IPG strips can serve as bridge.

3.1.4 Sample application

It was further investigated whether the position of sample application affects the quality of the resulting 2D gels. Figure 8 shows that protein migration during IEF is independent from sample application point. We took 24 cm commercial linear pH 4–7 IPG gel (Amersham Bioscience) and cut them into a 16 cm piece with a calculated pH range from 4–6 and an 8 cm piece with a calculated pH range from 6–7. The 2D PAGE pattern of the pH 4–6 gel was almost identical

independent of sample loading position (the acidic or the basic IPG strip). Thus, the point of sample application for daisy chain IEF affects results only marginally. Nevertheless, optimization for each particular sample is necessary (Gorg et al., 2004). In this experiment, we use a few drops of electrophoresis grade agarose gel to form the bridge between adjacent IPGs. Agarose gel was applied directly upon the bridging point of strips under oil. Although agarose bridges have excellent protein transfer properties, they are often associated with smearing artifacts in IEF as demonstrated in Figure 8.

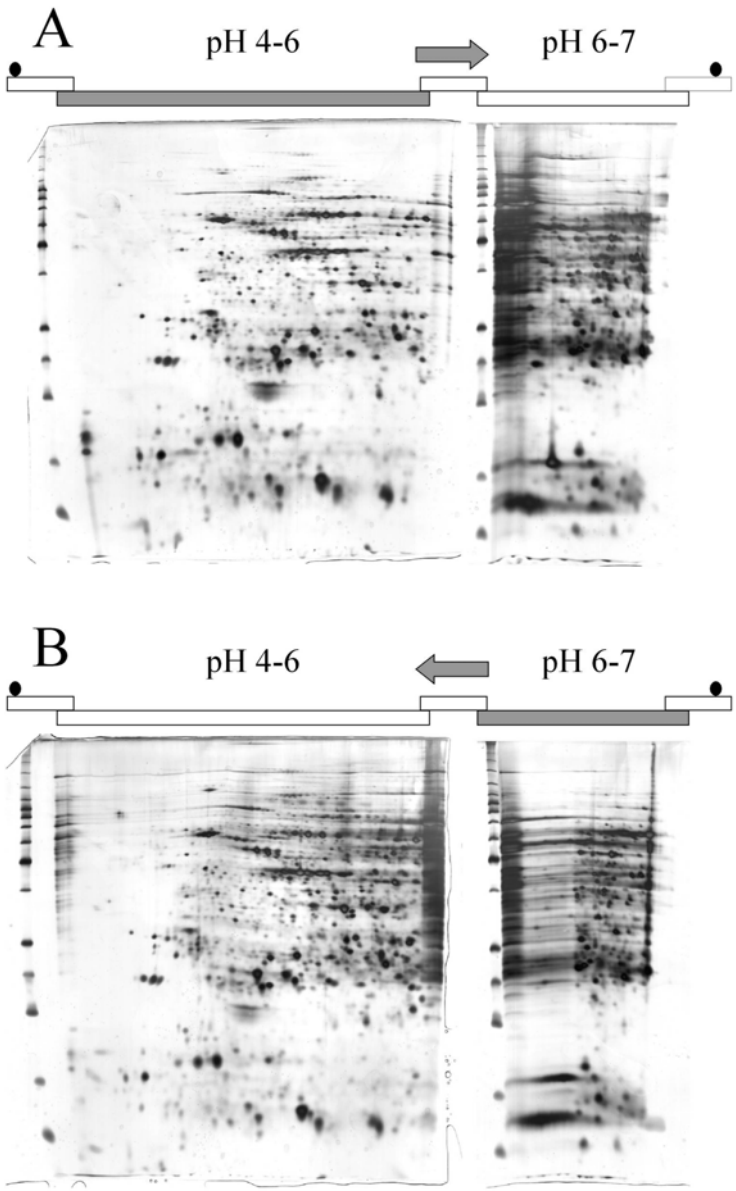

Figure 8: Electrophoretic pattern is same independent of sample application point in the daisy chain experiment. (A) sample was loaded by rehydration to the acidic IPG strip or (B) to the basic IPG.

3.1.5 Protein pattern

The quality of 2-D PAGE obtained in our experiments with serial IPG "daisy chain" IEF were by no means worse than those obtained when the same sample was analyzed on individual single IPGs, as shown in Figure 9. The quality of the singly electrophoresed pH 4–5 gel shown at Figure 9B was unusually poor in this particular experiment. Nevertheless, this result was obtained in triplicate using the same buffers and IPG batch as the daisy chain gel shown at Figure 9A that was also made in triplicate.

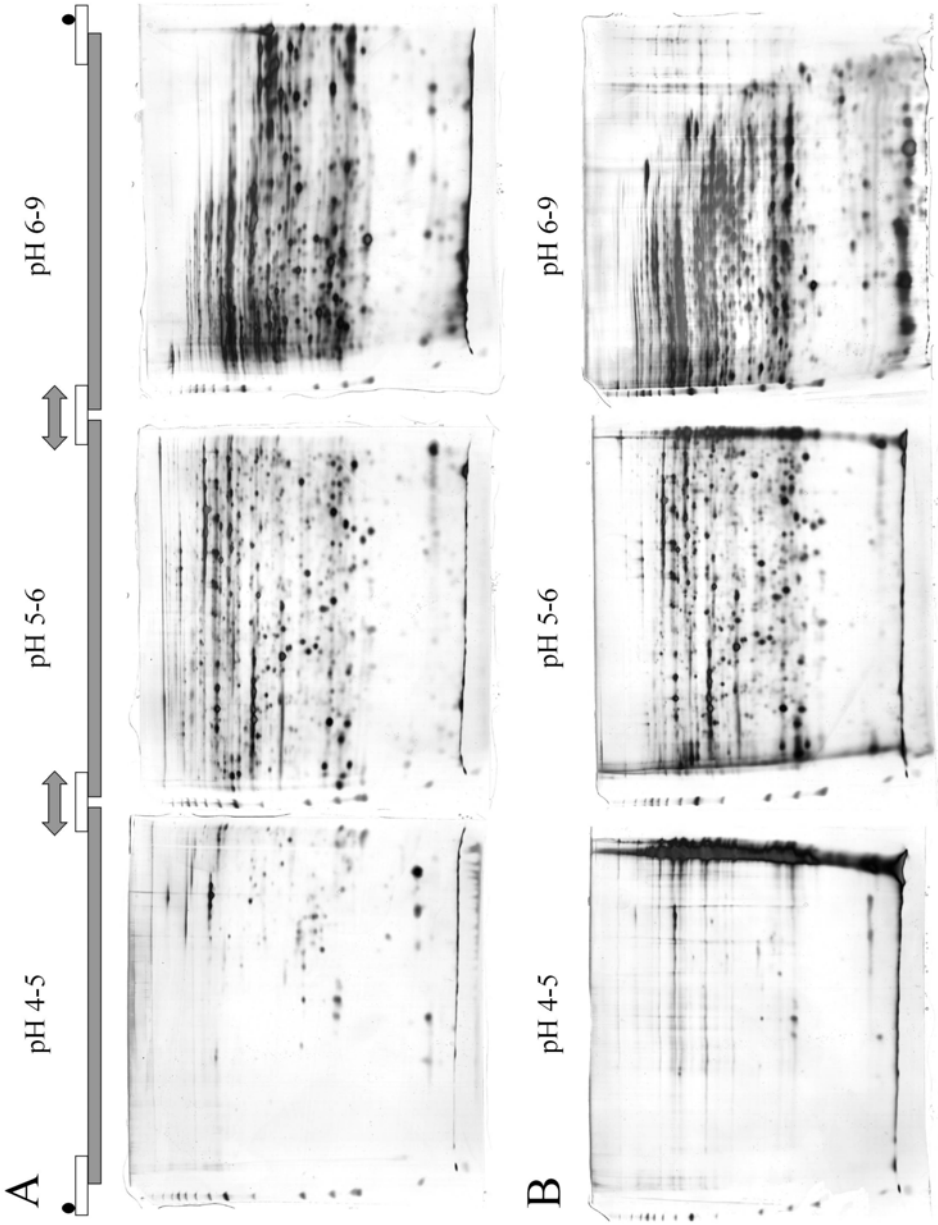

Figure 9: The quality of 2-D PAGE obtained with serial IPG "daisy chain" IEF were by no means worse than those obtained when the same sample was analyzed on individual single IPG. 200 µg of swine liver protein was applied to the serial IPG (A) and in (B) 250 µg of protein was loaded separately on each IPG.

It was found out that poor quality results are often obtained after rehydration loading of IPGs of extremely acidic or extremely alkaline pH. The pH 6–9 single IPG (Figure9B) was electrophoresed in SDS-PAGE in a separate experiment than the other gels in the figure.

3.1.6 Continuity of pH gradient

Next, parameters were investigated, which are associated with continuity of the pH gradient, and which are not relevant to other types of IEF. As shown in Figure 6 we found that a gap in the pH gradient did not adversely affect IEF, e.g., omitting the middle pH 5–6 IPG would not greatly affect the 2D PAGE patterns generated by the pH 4–5 and pH 6–9 IPGs. Proteins with pI between pH 5 and 6 accumulate in the bridge, and could be harvested and subjected to further separation steps if desired (not shown).

I investigated as well the effect of overlapping pH regions. Serial IEF of IPGs covering ranges of pH 4–7 and pH 6–9 creates an overlap in the pH region 6–7, which is present on both IPGs. Under these conditions we observed protein streaking in the IEF of the overlapping pH region on both IPGs (Figure 10A). Proteins were loaded to the acidic IPG by in-gel rehydration. For a control of this streaking effect, due to the overlap of pH ranges, we truncated an 18 cm pH 6–9 IPG to approximately pH 7–9 by cutting 6 cm from the acidic end.

By thus eliminating the overlap of pH ranges between IPGs, the streaking was eliminated (Figure 10B). We did not investigate the causes of this phenomenon further; however it could be due to decreased buffer capacity of the carrier ampholytes. With this experiment, we concluded that overlapping pH-buffering capacity in the individual IPGs has a deleterious effect on serial daisy chain IEF. On the other side, gaps in the pH range can be tolerated if desired.

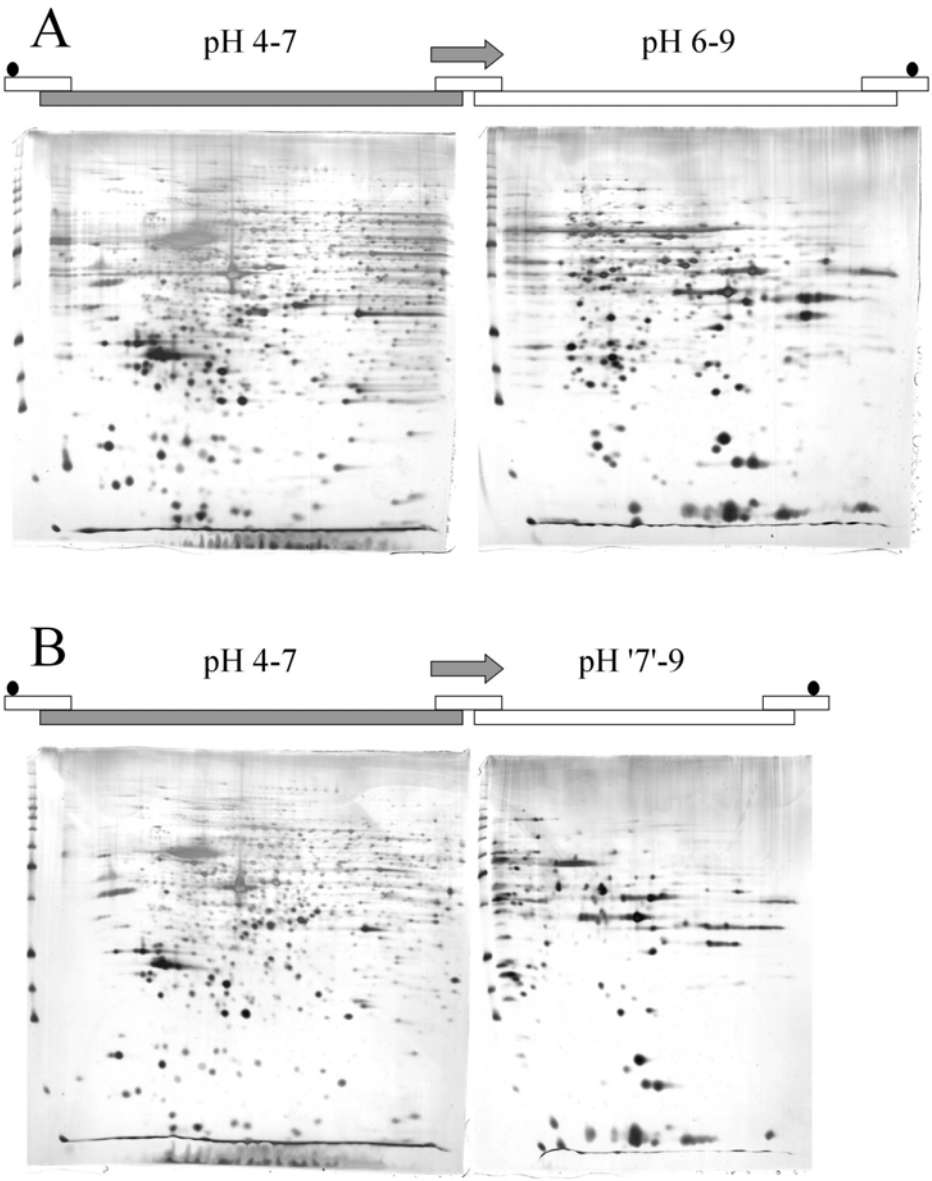

Figure 10: Quality of 2D PAGE pattern deteriorate when overlapping pH regions in serial IPGs was used. (A) overlapping pH region (B) consecutive

3.2 Biological application

3.2.1 Differential Radioactive Proteomic Analysis of Microdissected Renal Cell Carcinoma

3.2.1.1 ProteoTope analysis of RCC

Both cancerous cells and healthy cells sample were aliquoted into two fractions, which were each radiolabeled with either ^{125}I or ^{131}I. Samples were then cross-mixed with inversely labeled proteins of the opposite sample, and subjected to complementary replicate 54 cm IPG IEF daisy chain gels (pH 4-9) as shown in Figure 11.

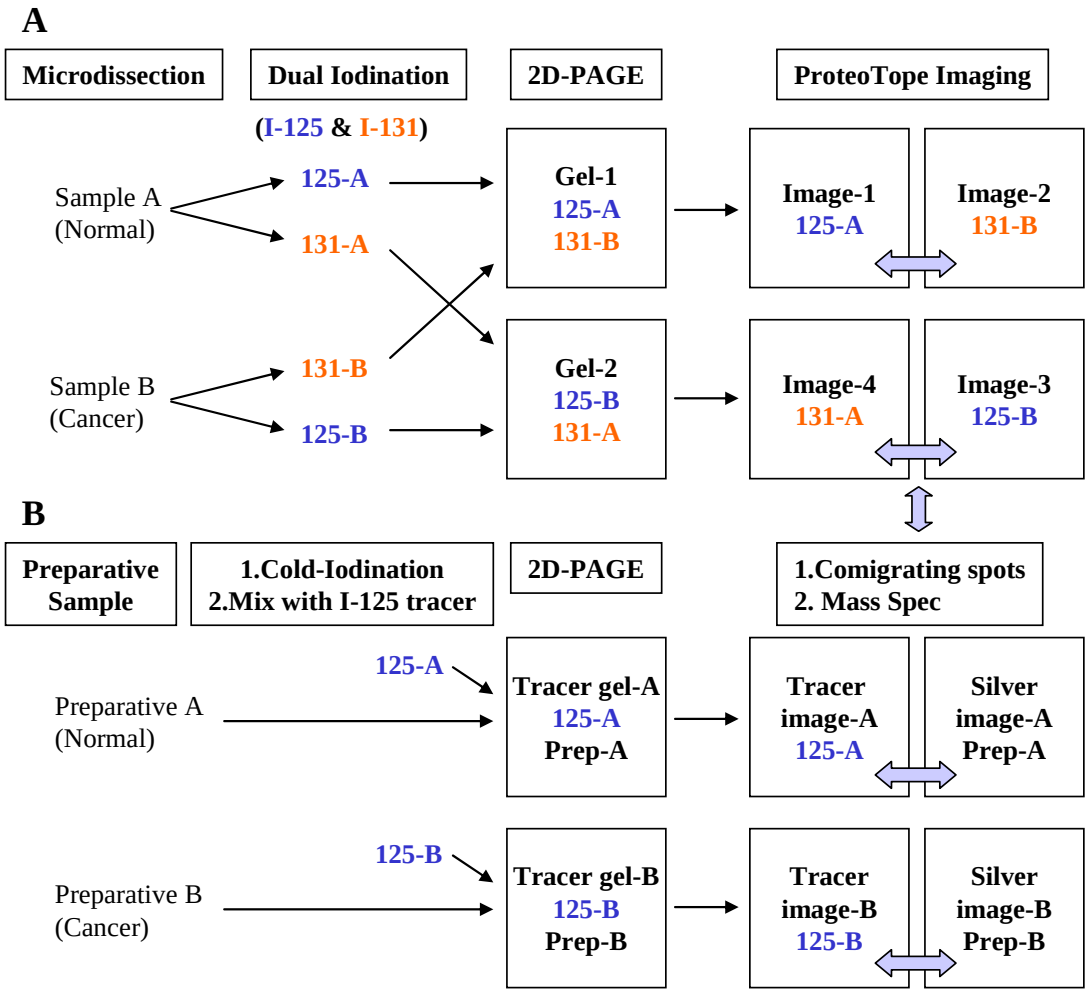

Figure 11: ProteoTope inverse replicate and tracer gel experimental design.

All gels were run in duplicate. Each sample (normal and cancer) was separately iodinated with each of two radioactive iodine isotopes: ^{125}I (blue) and ^{131}I (orange) (Figure 11A). The radioactively labeled proteins were mixed together

and run on inversely labeled replicate gels. For the analysis of comigrating spots I prepared tracer gels (Figure 11B). Preparative amounts of protein were separately iodinated non-radioactively, mixed with trace of radiolabeled samples 125-A and 125-B and run together in 2D-PAGE (Figure 11B). Resulting radioactive 2D-PAGE image was silver stained and matched to image from A. Comigrating spots with ^{125}I labeled proteins of interest were identified with mass spectrometry (Poznanovic et al., 2005b).

False color images of analytical ProteoTope gels are shown in Figure 12. First two panels represent the individual grayscale signals for both iodine isotopes that were measured (normal tissue labeled with ^{125}I and cancer tissue labeled with ^{131}I) and bottom ones show the corresponding dual isotopic channel multiplexed images of all inverse replicate gels. In the duplicate serial IPG-IEF gel pair of Gel-1 and Gel-2, normal tissue sample is labeled with ^{125}I and cancer tissue sample with ^{131}I. In contrast, in the inverse replicate labeled gel pair of Gel-3 and Gel-4 normal tissue sample was labeled with ^{131}I and cancer tissue sample with ^{125}I.

In the each of the multiplex images, protein spots labeled with pure ^{125}I are represented with false blue color and pure ^{131}I labeled protein spots are presented with false orange color. Equal amounts of both isotopes produce a gray or black color.

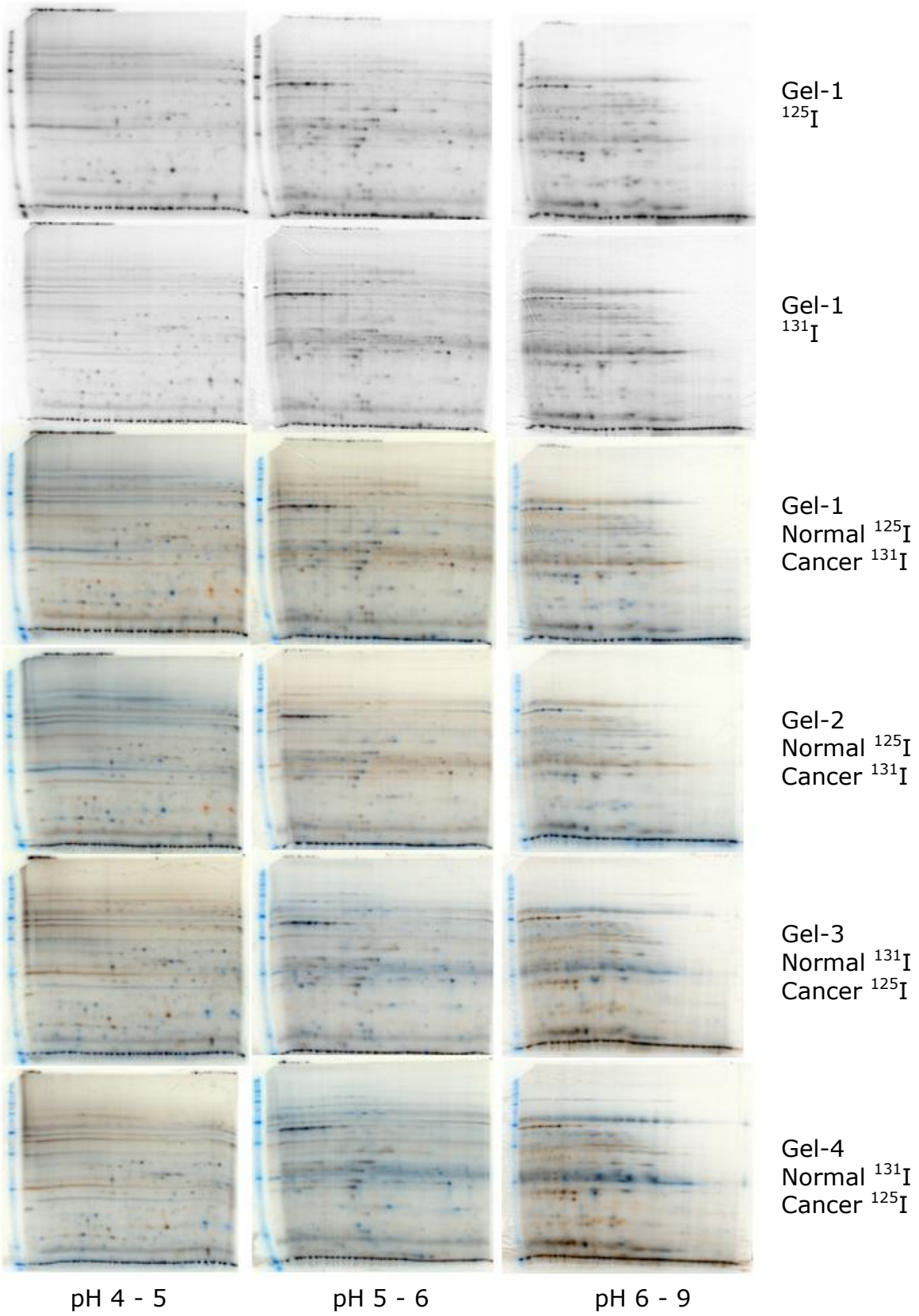

Figure 12: Differential ProteoTope analysis of microdissected samples. In each multiplex image. Pure ^{125}I produce blue color, pure ^{131}I produces orange color, and equal mixtures of calibrated signal from both isotopes produces gray or black color

Spots were quantified with the GREG software after differential ProteoTope measurement. The differential ratios were normalized by conversion to log odds values and statistically analyzed. Resulting synthetic average daisy chain ProteoTope gels are shown in Figure 13. All images were aligned with the images from the preparative tracer gels, those containing a trace of ^{125}I-labeled sample mixed with 240 µg cold labeled preparative sample from whole cryo-slices of cancerous or normal tissue. Blue color represents normal and orange cancer; spots were detected across all four gels from Figure 12.

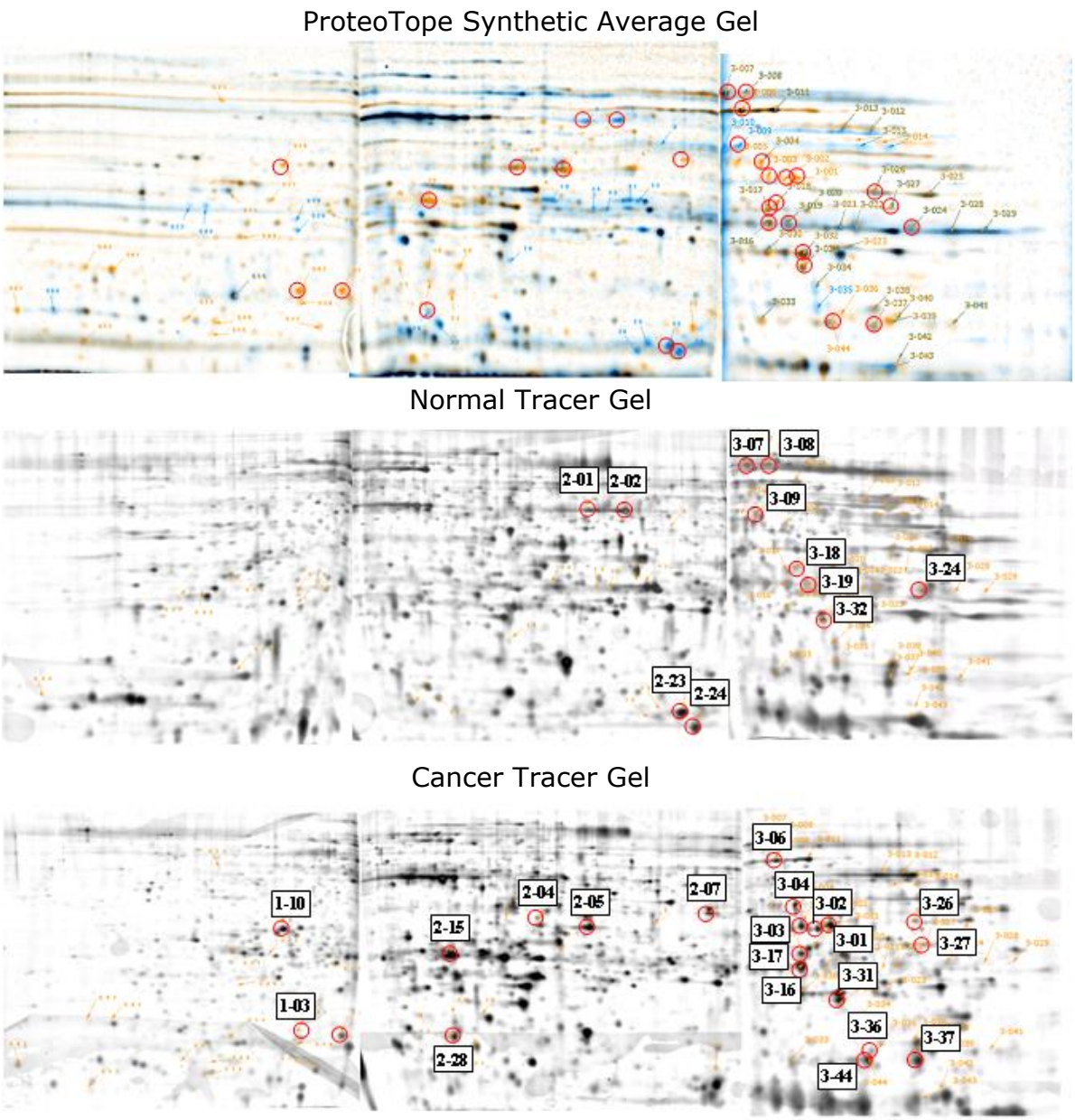

Figure 13: Protein identification. The top panel - synthetic average ProteoTope gel. Middle and lower panel - the position of differentially identified proteins on preparative gels loaded with Normal and Cancer tissue sample.

3.2.1.2 Mass Spectrometry

Tracer gels were performed in duplicate for each experimental condition (normal and cancer) and only one gel from each condition was subsequently used for mass spectrometry-based identification (Figure 13). Among differential proteins detected by ProteoTope quantification from 3.8 µg microdissected tissue, only 29 proteins were unambiguously comigrating with the radioactive tracer, and were more than 2-fold differentially abundant at the 5% significance level. These spots were excised, digested with trypsin and identified by MALDI-TOF-MS peptide mass fingerprinting (PMF) with PMF scores >70. The mass spectrometry results are summarized in Figure 14.

Spot Nr.	Protein	NCBI Accession	PMF score	Cancer (%)	StdErr (%)	p-value	0 50 100
2-23	M-FABP / MDGI	gi|227994	82	0.0	0.0	**<0.0001**	
2-24	L-FABP	gi|4557577	98	0.0	0.0	**<0.0001**	
3-09	aldo-keto reductase family 1, member A1	gi|5174391	132	5.9	2.8	0.0102	
2-01	aminoacylase 1	gi|4501901	136	10.6	1.1	**0.0003**	
2-02	aminoacylase 1	gi|4501901	193	15.9	5.7	0.0270	
2-28	transthyretin	gi|2098275	124	21.1	3.3	**0.0066**	
3-19	Ig kappa chain V-III	gi|106586	66	24.7	4.0	0.0137	
3-24	glutathione transferase omega-2	gi|345859	73	33.7	1.8	**0.0032**	
3-37	Peptidylprolyl isomerase A	gi|13937981	96	65.8	1.9	**0.0046**	
3-27	galactose-specific lectin	gi|1196442	131	69.3	4.7	0.0323	
3-18	carbonic anhydrase I	gi|4502517	140	72.7	3.8	0.0133	
3-07	aldehyde dehydrogenase 1	gi|2183299	141	74.9	4.0	0.0134	
3-08	pyruvate kinase 3 isoform 1	gi|33286418	224	75.2	5.6	0.0291	
3-17	Phosphoglycerate mutase 1	gi|38566176	149	75.6	4.3	0.0150	
3-32	Manganese superoxide dismutase	gi|34707	108	76.5	1.2	**0.0004**	
3-44	Peptidylprolyl isomerase A	gi|1633054	88	78.5	1.1	**0.0003**	
3-31	crystallin, alpha B	gi|4503057	194	82.9	2.8	**0.0039**	
2-05	Annexin A4	gi|1703319	144	82.9	1.4	**0.0005**	
3-16	triosephosphate isomerase 1	gi|4507645	161	84.5	1.2	**0.0003**	
3-26	carbonyl reductase 1	gi|4502599	164	85.3	3.1	**0.0048**	
2-04	Annexin A4	gi|1703319	77	88.8	0.2	**<0.0001**	
1-10	Actin B	gi|15277503	125	90.8	1.8	**0.0016**	
1-04	Annexin V	gi|809185	149	97.1	1.0	**0.0016**	
2-15	Heat shock protein 27	gi|662841	146	97.6	0.6	**0.0005**	
1-03	Annexin V	gi|809185	197	100.0	0.0	**<0.0001**	
2-07	phosphoglycerate kinase	gi|4505763	73	100.0	0.0	**<0.0001**	
3-01	glyceraldehyde-3-phosphate dehydrogenase	gi|31645	152	100.0	0.0	**<0.0001**	
3-03	glyceraldehyde-3-phosphate dehydrogenase	gi|31645	132	100.0	0.0	**<0.0001**	
3-04	Aldo-keto reductase family 1, member B1	gi|4502049	116	100.0	0.0	**<0.0001**	
3-06	enolase 1	gi|4503571	223	100.0	0.0	**<0.0001**	
					Colour code:	**Normal**	
						Cancer	

Figure 14: ProteoTope analysis of microdissected renal cell carcinoma: List of identified significantly differential proteins.

3.2.2 Breast cancer proteomics by laser capture micro dissection

3.2.2.1 Sample pooling and ProteoTope analysis

Our previous results have shown that for reliable analysis of LCM samples with 2D-PAGE, following radioiodine labeling, higher amounts of protein were required, than typically obtained from approx. 10,000 laser pulses. For this purpose we developed a sample pooling strategy to enable ProteoTope analysis of microdissected protein samples from well-characterized cell populations of breast cancer. Between various possible pooling strategies we chose the design shown in Figure 15.

Performance of this pooling method was tested using LCM-harvested proteins from breast tumors that were pooled on the basis of being either estrogen receptor positive / progesterone receptor positive (ER+/PR+) or estrogen receptor positive / progesterone receptor negative (ER+/PR-) as it shown in Table 3

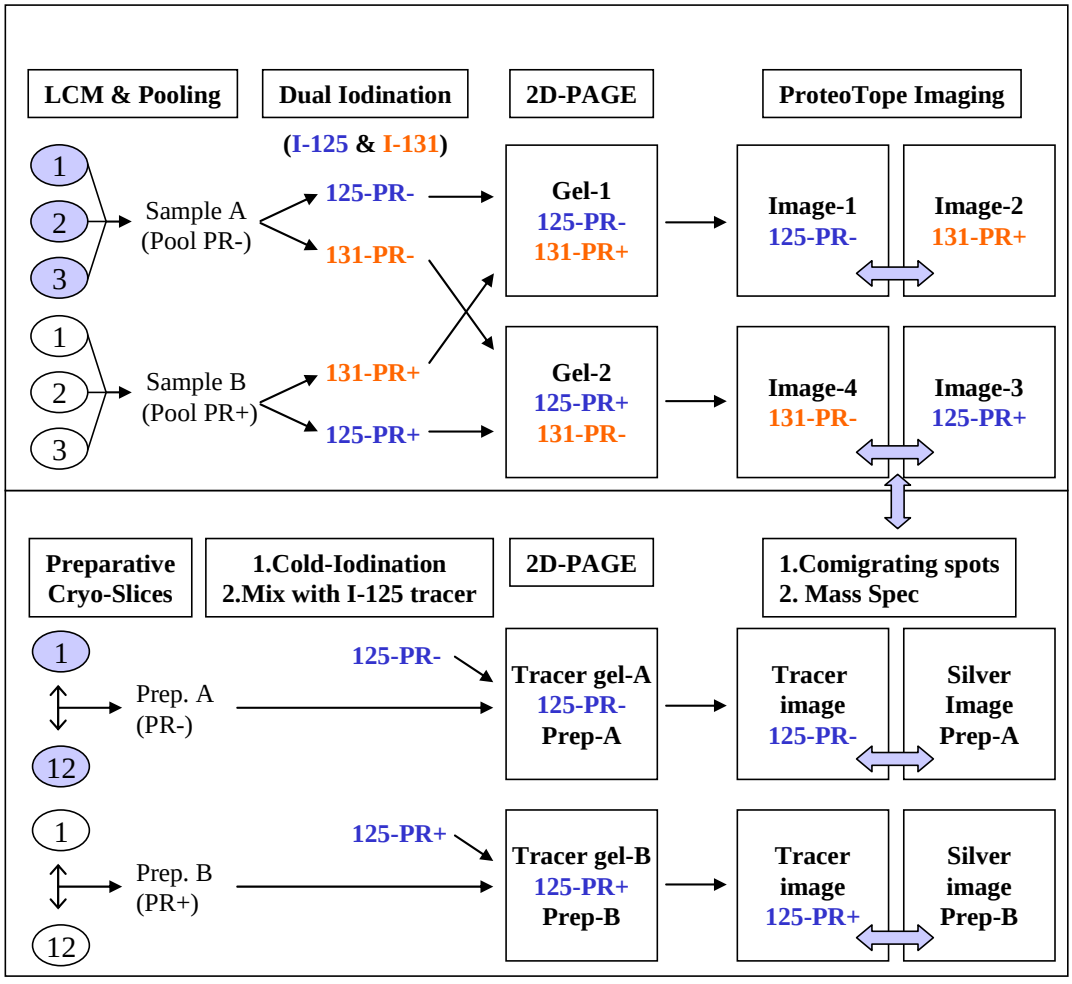

Figure 15: Breast cancer sample pooling strategy

The quality of each tumor sample was checked by determining integrity of RNA with Agilent Bioanalyzer prior to protein analysis. Only tumors with intact 18S and 28S ribosomal RNA were included in study. Frozen tumor sections were dehydrated as described (Wulfkuhle et al., 2002). One section was stained with haematoxylin/eosin, and cancer cells suitable for laser microdissection were identified. From each tumor sections were taken 10,000 shots of a 30 µm laser diameter with laser capture microscope. The micro-dissected tissue was extracted directly into iodination buffer, and treated as described in the material and methods. After harvesting samples, two main groups were assigned. First, with twelve ER+/PR+ tumors and second with twelve ER+/PR- tumors. Every of these groups consist of four subgroups of three tumors each, and they belong to one sub-pool. Each sub-pool contains equal LCM shot equivalents as it shown in Table 3 and described in the material and methods. (Table 3) also provides additional information of the clinical parameters associated with each analyzed tumor.

For ProteoTope differential analysis, samples from three separately LCM harvested ER+/PR+ (PR+) or ER+/PR- (PR-) tumors, were mixed and aliquots of the pooled sample were iodinated with ^{125}I (blue) and ^{131}I (orange) (Figure 15). The radioactively labeled samples were mixed together and run on inversely labeled 2D-PAGE. For the tracer gels, preparative amounts of protein were obtained from 35-45 different cryogenic slices from all 12 tumors (Table 3). Pooled protein samples were iodinated non-radioactively and mixed with a trace of radioactive labeled protein from a pool of all four samples labeled with ^{125}I and run in 2D-PAGE.

In Figure 16 an example result of one inverse replicate differential ProteoTope analysis is shown. For every gel we needed 5% (approx. 180 ng) of the radioactively labeled protein pool, labeled in the inverse replicate control design shown in Figure 15. This pooling strategy was giving us ample material to repeat any 2D-PAGE experiment for up to several weeks if necessary.

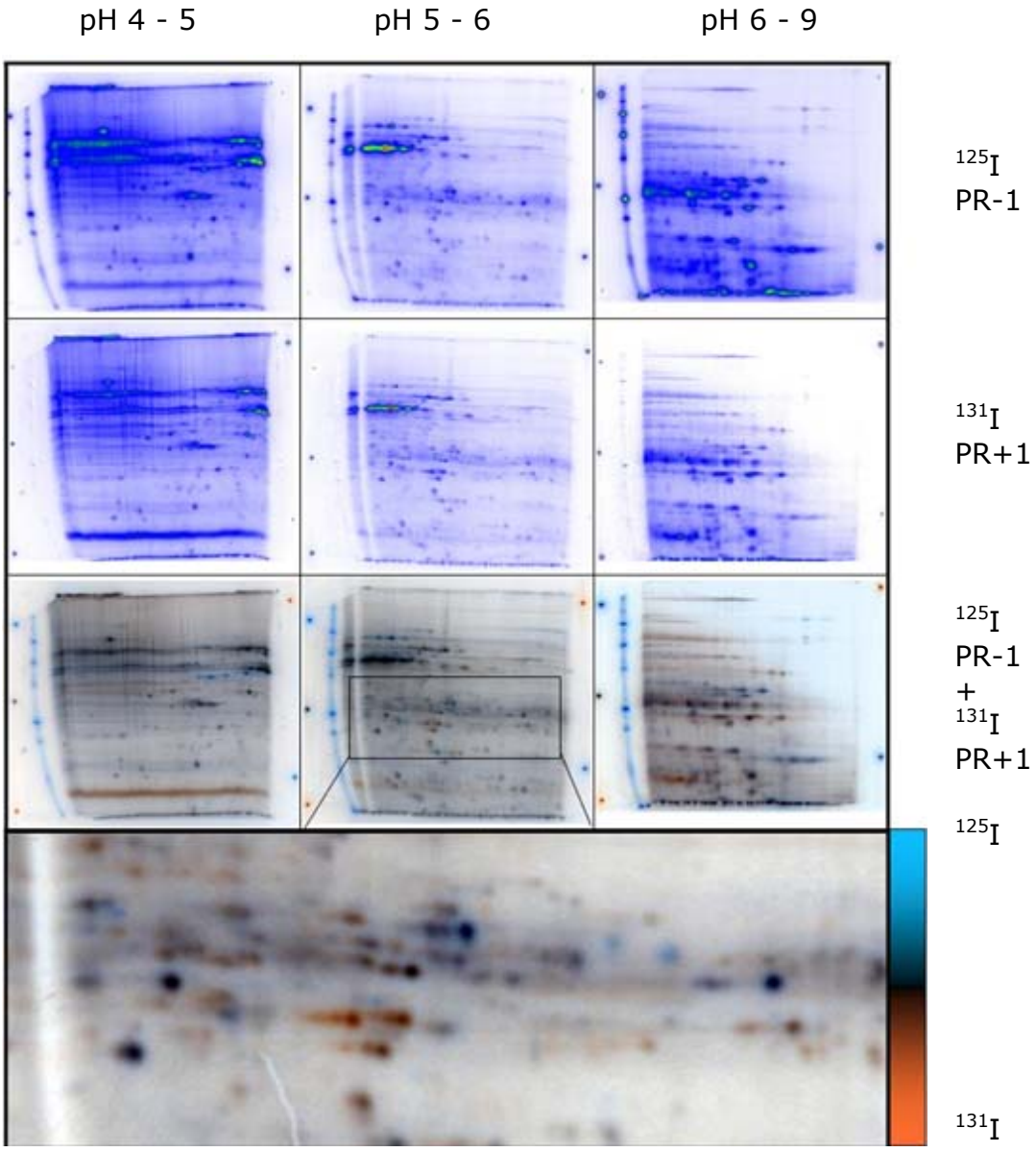

Figure 16: Example of inverse replicate differential ProteoTope analysis of pooled LCM breast cancer samples.

The 2D-PAGE patterns obtained were not as reproducible for these gels as for those obtained when more protein per iodination reaction was available e.g.(Schrattenholz et al., 2005; Poznanovic et al., 2005b). This is probably because of greater variability in sample preparation due to the extremely low amounts of source protein. All images have shown similar striking and there were relatively few consistent differences between these samples, and which is in line with the fact that all tumors in this analysis possess the ER. This can be seen from the synthetic average gels in Figure 17.

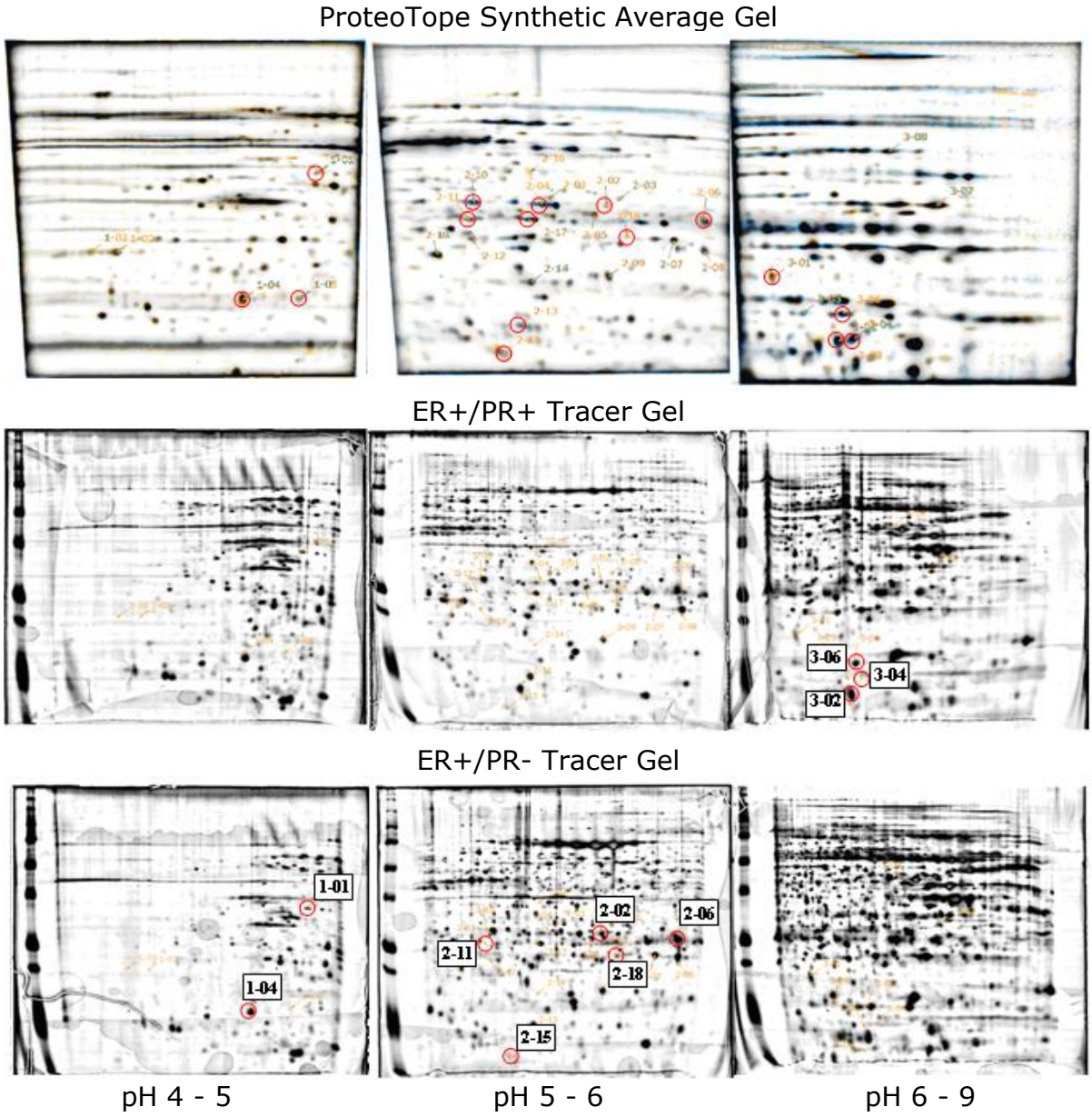

Figure 17: Protein identification**.** Synthetic average (top panel) and preparative tracer gel (lower two panels) with differentially identified proteins.

The synthetic gel image in Figure 17 was computer-generated produced by matching spots across gels, and their intensities were statistically analyzed relative to their PR status. This figure also shows preparative silver-stained gels that were loaded with proteins from the pooled whole tissue slices from each test condition (Table 3). The silver stained gel images were used for protein localization and identification. In Figure 18 MALDI-TOF-MS peptides mass fingerprinting data of identified proteins are shown that were consistently and significantly differential between ER+/PR+ and ER+/PR- tumors from the ProteoTope analysis of all four pools.

Prot. Nr.	Protein	GenBank Identity	PMF Score	ER+/PR+ (%)	StdErr (%)	p-value	0 50 100 (%)
2-02	n.i.			21,7	5,2	0,023	
1-04	microsomal cytochrome b5	gi|353818	105	26,9	3,7	**0,006**	
2-06	immunoglobulin kappa light chain	gi|21669479	73	35,8	4,1	0,045	
3-01	transgelin; SM22-alpha	gi|4507359	113	36,6	4,3	0,039	
2-15	n.i.			37,3	3,4	0,036	
1-01	eukaryotic translation EF 1 delta isoform 2	gi|4507359	88	38,4	3,3	0,027	
2-11	n.i.			38,8	2,4	0,019	
2-18	glutathione S-transferase	gi|2204207	84	39,1	2,6	0,028	
1-05	SPUF/Neudesin	gi|7019545	82	59,9	1,3	**0,002**	
2-10	cathepsin D preproprotein	gi|4503143	95	62,0	0,5	**<0.001**	
3-04	n.i.			62,5	2,9	0,014	
2-04	n.i.			63,5	3,5	0,035	
3-02	Hemoglobin beta chain	gi|1942686	104	65,0	1,8	**0,002**	
3-06	peptidylprolyl isomerase A isoform 1	gi|10863927	93	65,8	2,1	**0,002**	
2-17	n.i.			72,8	2,3	**0,003**	
2-13	Cellular Retinoic-Acid-Binding Protein Type II	gi|999882	76	77,3	1,0	**<0.001**	

Colour code: ER^{+}/PR^{-} ER^{-}/PR^{-}

Figure 18: List of identified proteins for breast cancer sample that differ significantly by more than 1.5 fold on average

3.2.3 Comparative Profiling of the Mammalian Mitochondrial Proteome

To come to a conclusion about the requirements concerning the differential analysis of age-related oxidative posttranslational modifications of mitochondrial proteins, we performed a comparative proteomic study, using a uniform standard preparation of bovine heart mitochondria (Figure 19).

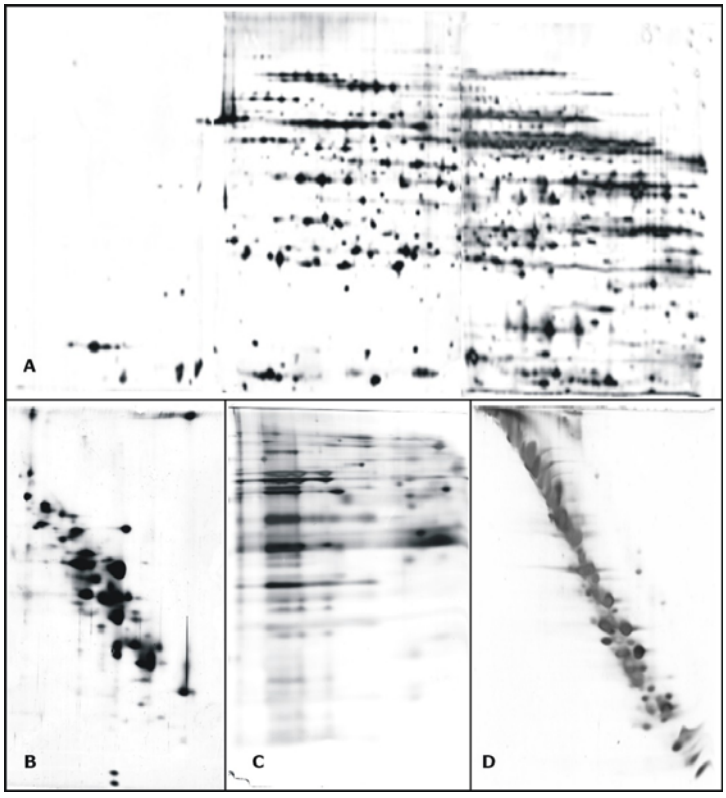

Figure 19: Four different SDS-2D-PAGE methods for separation of bovine heart mitochondria. (A) 54 cm IPG-IEF Daisy chain pH 4-9, (B) Tricine-urea/Tricine, (C) blue native SDS 2D PAGE, (D) 16-BAC SDS 2D PAGE

For the comparison of methods to differentially investigate age-related oxidative changes in mitochondrial proteins, the following first dimension separations prior to second dimension SDS-PAGE were employed: high resolution 54 cm serial IPG-IEF daisy chain (Poznanovic et al., 2005a) (Figure 19A), tricine-urea/tricine (Rais et al., 2004) (Figure 19B), blue native (Brookes et al., 2002; Krause et al., 2005; Schagger, 2001) (Figure 19C), and 16-BAC (Hartinger et al., 1996) (Figure 19D). As one can see the resolution of an identical sample from bovine heart mitochondria preparation obtained by high resolution 54 cm serial IPG-IEF-SDS-PAGE (daisy chain) is far superior to all other methods. As shown the (Table 4) number of detected spots, vary among different methods from the

same preparation of bovine heart mitochondria. The highest number of detected spots was seen by IPG-IEF-SDS-PAGE total of 1008 spots, following by blue native/SDS-PAGE 172 spots, 16-BAC/SDS-PAGE 121 spots and tricine-urea/tricine-SDS-PAGE 117 spots (Table 4). It should be noted that only separated proteins have a chance to be differentially quantified.

	IEF/PAGE	Blue native	16-BAC	Tricine-urea
Detected spots	1008	172	121	117
Picked spots	745	160	106	80
Identified proteins	400	152	67	55
Nonreduntant proteins	123	71	30	41
Exclusive proteins	80	23	6	10

Table 4: The number of spots detected and subsequently identified with MALDI-TOF Peptide Mass Fingerprinting, from a uniform preparation of bovine heart mitochondria

Proteins found in	IEF-PAGE	Blue native	16-BAC	Tricine urea	Joint ID's	Total
four methods	x	x	x	x	6	6
three methods	x	x		x	11	17
	x	x	x		4	
		x	x	x	1	
	x		x	x	1	
two methods	x	x			11	32
	x			x	5	
	x		x		2	
		x		x	5	
		x	x		8	
			x	x	1	
one method	x				80	119
		x			23	
				x	10	
			x		6	
Total						174

Table 5: Distribution of identified nonredundant proteins found in four different separation methods

Our intention was not to identify all visible spots, but only those that were medium to high abundant and were easily accessible for automated procedure of detection and identification. In total detected 1418 spots were using the Greg software. From this number 1091 spots were picked and 674 spots were identified (Table 4). As shown in Table 5 a total of 174 nonredundant proteins were identified among all methods and nonredundant proteins that were detected in only one of the methods were called "exclusive" proteins. Our main focus in this study was on a uniform sample for all methods, not on being comprehensive and

for sure many more proteins could have been identified with appropriate effort (Hunzinger et al., 2006; Devreese et al., 2002; Rais et al., 2004; Zahedi et al., 2005).

The comparison of the four methods with regard to separation of age-related posttranslational modifications induced by reactive oxygen species (ROS) (Soskic et al., 2007) shows that resolution is the key issue. We found only 6 non-redundant proteins in all four methods, 17 proteins were found in only three methods, 32 were found in only 2 methods and the remaining 119 were found by only one method (80 of these were found in IEF/PAGE (Table 4). Between the six non-redundant proteins identified by all four methods, there are two subunits of the ATP-synthase complex, two further proteins from the respiratory chain and in particular two mitochondrial citric acid cycle enzymes: aconitase-2 and NADP+-dependent isocitrate dehydrogenase (IDPm) (Table 6).

accession	Description	theoretical		IEF-PAGE		blue native	tricine-urea	16-BAC
		Mw	pI	Mw	pI	Mw	Mw	Mw
gi|27806769	Aconitase 2, mitochondrial [Bos taurus]	87606	8.1	93000 93000 92000 92000 92000 92000 92000 92000 91000	6.5 6.55 6.6 6.7 6.8 6.9 7.0 7.1 7.2	93000 88000	66000	92000 83000
gi|27807143	Ubiquinol-cytochrome c reductase core protein II [Bos taurus]	48473	9.1	45000 45000 45000 45000	6.6 6.8 7.1 7.3	53000 51000 50000	41000 41000	45000 43000 43000 41000
gi|27807355	NADH dehydrogenase (ubiquinone) Fe-S protein 1, 75kDa (NADH-coenzyme Q reductase) precursor [Bos taurus]	79391	6.1	80000 80000 79000 79000 79000 78000 77000 76000	5.15 5.2 5.25 5.3 5.35 5.4 5.45 5.5	77000	61000 59000	83000 74000
gi|28461205	Isocitrate dehydrogenase 2 (NADP+), mitochondrial [Bos taurus]	52209	9.1	44000 44000	8.1 8.3	50000	42000 41000	54000 41000
gi|27807237	ATP synthase, H+ transporting, mito-chondrial F1 complex, alpha subunit [Bos taurus]	59683	9.7	56000 56000 55000 55000	7.2 7.4 6.9 7.0	61000 60000 59000 54000	66000 50000 50000	55000 53000 55000 52000
gi|28461221	ATP synthase, H+ transporting, mito-chondrial F1 complex, beta subunit [Bos taurus]	56249	4.8	54000 53000 53000 53000 50000 50000	4.95 5.0 5.05 5.1 4.9 4.95	57000 56000 46000 39000	49000 48000 46000 45000	52000 50000 49000 40000 39000 38000 27000 26000

Table 6: Analysis of 6 non-redundant proteins found by all four methods

The latter two recently have been implicated in oxidative stress regulation and related diseases (Shadel, 2005; Yarian et al., 2005; Chen et al., 2005; Yang et al., 2005; Jo et al., 2001; Kil et al., 2004a; Kil and Park, 2005; Kil et al., 2004b; Bulteau et al., 2005). NADP+-dependent isocitrate dehydrogenase plays a role as one of the main sources of NADPH, it is cofactor in many biosynthetic pathways and particularly in the regeneration of reduced glutathione which is critically important in cellular defense against oxidative damage (Jo et al., 2001; Kil et al., 2004a; Kil and Park, 2005; Kil et al., 2004b; Bulteau et al., 2005). It was found that modulation of IDPm is an age-dependent and a tissue-specific phenomenon (Kil et al., 2004b). We found variety of IDPm isoforms across all used methods but their distinct molecular features were not investigated further. On the other side, having in mind, that for all methods we used a uniform sample preparation of bovine heart mitochondria, it was interesting to explore the number and nature of redundant spots and their respective relevance for ROS-mediated posttranslational modifications. One of these spots was aconitase-2, therefore it was of interest to focus on a more detailed molecular analysis of the 14 isoforms of aconitase-2, which were found mainly by IEF/PAGE.

Aconitase-2 (EC 4.2.1.3) is an enzyme of the citric acid cycle in the mitochondrial matrix and belongs to the group of iron-sulfur proteins. It plays a unique role in age-related maintenance of mtDNA and has a unique pattern of expression during aging as compared to other mitochondrial proteins (Yarian and Sohal, 2005). A detailed analysis of non-canonical peptides of aconitase-2 peptides found in MALDI-TOF peptide mass fingerprints (PMF) gave indications of specific carbonylations, typical for age-related posttranslational modifications (Soskic et al., 2007).

One of these modifications was carbonylation (malondialdehyde) at lysine 700 (peptide 694-700, IHETNLmK MH+=916.849) predominantly found in two IEF/PAGE isoforms (92 kD, pI 6.8 and 6.9). This is in agreement with published data describing aconitase as a target for malonaldehyde modification (Yarian et al., 2005; Yarian and Sohal, 2005). Further, we identified two possible N-formylkynurenine modifications of two doubly oxidized tryptophan residues. One modification can be assigned at tryptophan 373 (peptide 371-378, EGfWPLDIR, MH+=1017.501) (Figure 20A). Second modification can be assigned to tryptophan 657 (peptide 657-671, fWVVIGDENYGEGSSR MH+=1699.756) (Figure 20B)

in both cases formylkynurenine is indicated as fW. Significant MS/MS data could not be obtained for unambiguous verification, but these peaks most likely represent the N-formylkynurenine modified peptides, since both modifications have been identified previously (Taylor et al., 2003a).

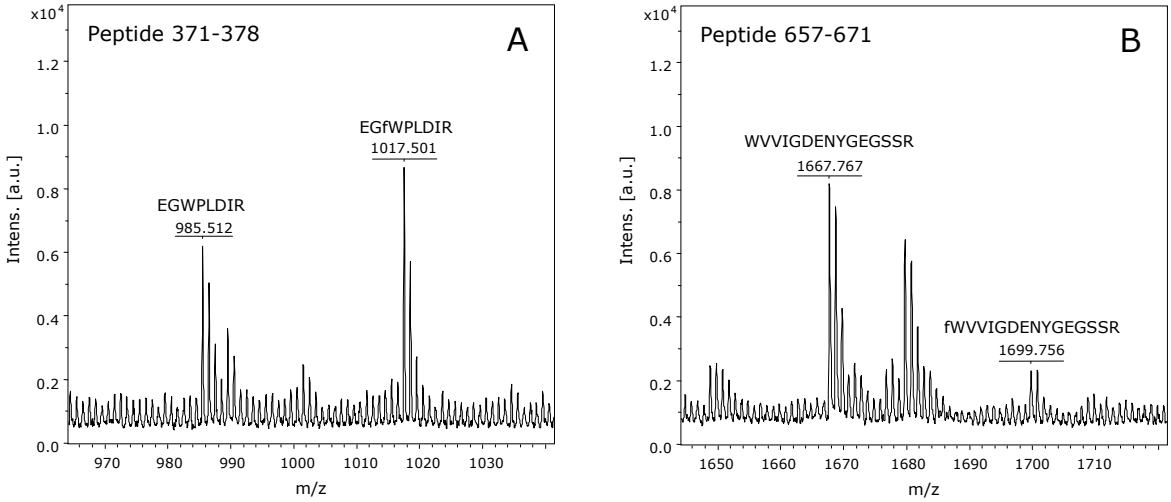

Figure 20: MALDI spectrum of unmodified and potentially N-formylkynurenine modified tryptic peptides (A) 371-378 (B) 657-671

For both sequences, we also found the unmodified peptides. The ratios of unmodified versus modified peptides were always <0 for peptide 371-378 (i.e., tryptophan 373 is predominantly oxidized) and >0 for peptide 657-671 (tryptophan 657 is predominantly nonmodified). Another aspect of this comparative study was to determine the very type of proteins recovered in each case: Mitochondria and in particular mitochondrial membranes have an exceedingly high percentage of membrane proteins. So a focus of the identification was on recovery of membrane proteins.

Integral membrane proteins are known for their generally poor solubility in IEF gels and have been broadly considered as difficult for standard 2D-PAGE. The blue native-PAGE (Rexroth et al., 2003), 16-BAC-PAGE (Hartinger et al., 1996), and tricine-urea/tricine-PAGE (Rais et al., 2004) have received particular attention as successful alternatives in some cases.

The hydrophobicity of a protein can be expressed using GRAVY plots (Kyte and Doolittle, 1982), which present average hydropathy score for all amino acids in a protein. Integral membrane proteins, as highly hydrophobic species have higher GRAVY scores than soluble proteins, typically >0. On the other side high

GRAVY scores can't reliably predict the structure without the help of hydropathy plots.(Kyte and Doolittle, 1982). To our surprise, under the condition used in this work, there was only a slight advantage for analyzing hydrophobic proteins using blue native and 16-BAC-PAGE as depicted in Figure 21 and Table 7. Proteins with GRAVY scores higher than 0.2 were almost exclusively found using blue native gels. But for proteins with GRAVY scores between 0.1-0.2, 2D-IEF-PAGE works notably well and with this method we detect more protein species with GRAVY scores >0 than with any other methods, among them unexpectedly quite a number of membrane proteins(Hunzinger et al., 2006).

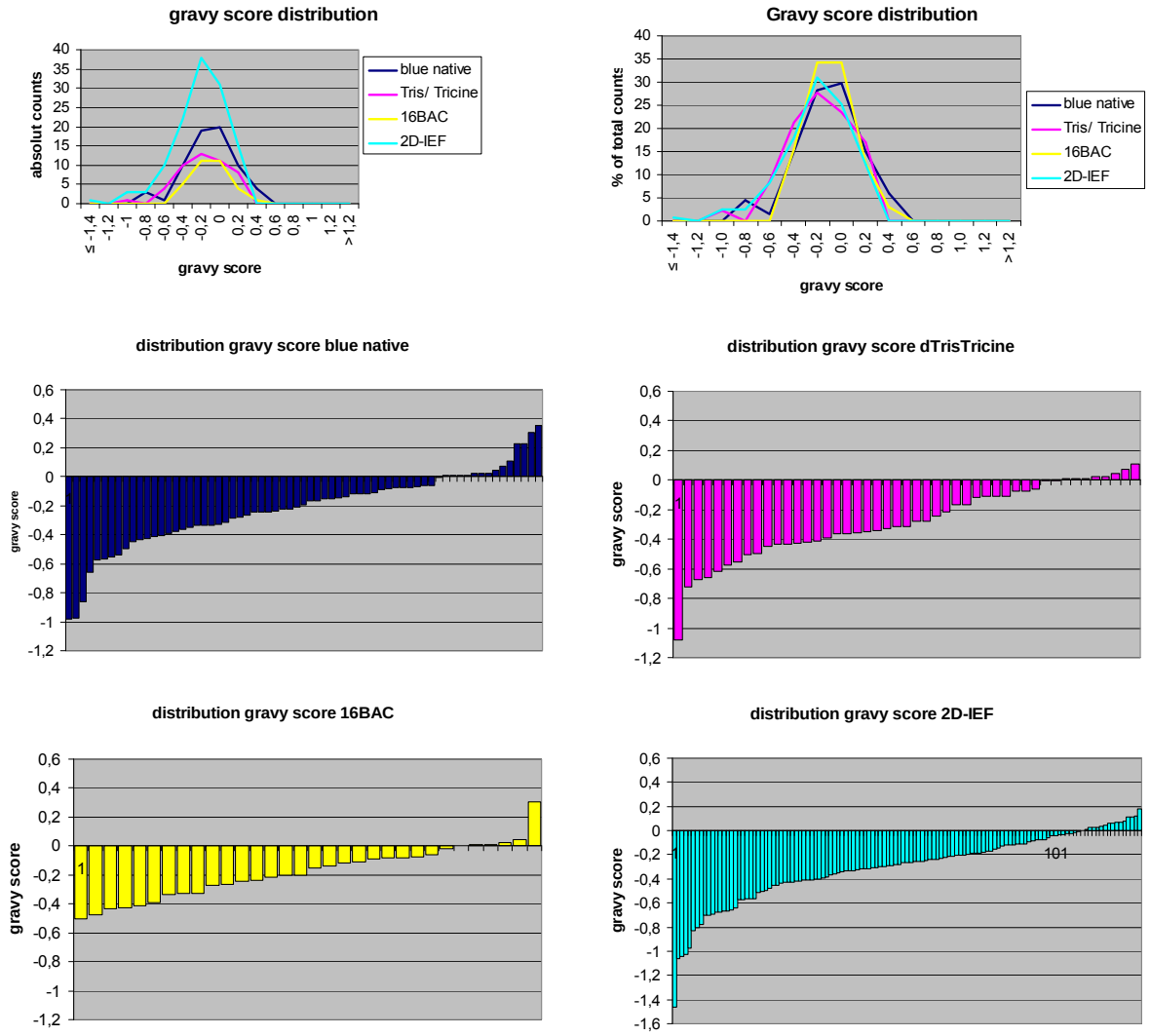

Figure 21: Histogram of GRAVY scores and GRAVY score distribution for all used methods

Identified proteins with positive GRAVY scores higher than 0 are listed in-Table 7. Among the 174 nonredundant proteins (GenBank entries) found in this

study, to our knowledge 14 have not been previously associated with mitochondria.

accession	pI	MW	description	GRAVY score	IEF-PAGE	blue native	tricine-urea	16-BAC
gi|27806831	8.3	113780	nicotinamide nucleotide transhydrogenase	0.305		x		x
gi|61866502	10.2	11409	PREDICTED: similar to ATP synthase, H+ transporting, mitochondrial F0 complex, subunit g	0.230		x		
gi|54310686	4.5	26004	cytochrome c oxidase subunit II [Bos grunniens]	0.225		x		
gi|27805907	8.5	27655	hydroxyacyl-Coenzyme A dehydrogenase, type II hydroxyacyl-Coenzyme A [Bos taurus]	0.183	x			
gi|61822295	10.1	15587	PREDICTED: similar to ES1 protein homolog, mitochondrial precursor (Protein KNP-I) (GT335 protein), partial [Bos taurus]	0.124	x			
gi|61863144	5.8	16782	PREDICTED: similar to FabG-like protein, partial [Bos taurus]	0.115	x			
gi|61867324	8.8	35646	PREDICTED: similar to Malate dehydrogenase, mitochondrial precursor [Bos taurus]	0.108	x	x	x	
gi|27805917	7.7	17490	histidine triad nucleotide binding protein 2	0.082	x			
gi|32189340	10.4	32946	solute carrier family 25 member 4 [Bos taurus]	0.076		x	x	
gi|27806561	6.5	37487	lactate dehydrogenase B [Bos taurus]	0.067	x			
gi|61842751	7.5	18936	PREDICTED: similar to serine/threonine/tyrosine kinase 1, partial [Bos taurus]	0.065	x			
gi|61553497	8.8	32286	mitochondrial short-chain enoyl-coenzyme A hydratase 1 precursor [Bos taurus]	0.061	x	x		
gi|28461221	4.8	56249	ATP synthase, H+ transporting, mitochondrial F1 complex, beta subunit [Bos taurus]	0.042	x	x	x	x
gi|448581	5.3	36828	pyruvate dehydrogenase:SUBUNIT=beta	0.031	x			
gi|27806307	10.6	23335	mitochondrial ATP synthase, O subunit [Bos taurus]	0.026	x	x	x	
gi|61831678	6.9	46913	PREDICTED: similar to Dihydrolipoamide dehydrogenase, precursor, partial [Bos taurus]	0.026		x		x
gi|59858383	6.5	36674	lactate dehydrogenase B [Bos taurus]	0.026		x		
gi|30583661	5.5	29786	prohibitin [Homo sapiens]	0.024	x		x	
gi|3660252	4.8	51397	Chain E, The Structure Of Bovine F1-Atpase Covalently Inhibited With 4-Chloro-7-Nitrobenzofurazan	0.011	x	x	x	x
gi|51247981	4.8	51673	Chain F, Beryllium Fluoride Inhibited Bovine F1-Atpase	0.011	x	x		x
gi|3660253	4.8	51449	Chain F, The Structure Of Bovine F1-Atpase Covalently Inhibited With 4-Chloro-7-Nitrobenzofurazan	0.008			x	
gi|11514059	4.8	51655	Chain D, Bovine F1-Atpase Inhibited By Dccd (Dicyclohexylcarbodiimide)	0.007	x	x	x	x
gi|61858852	9.1	45768	PREDICTED: similar to mitochondrial acetoacetyl-CoA thiolase, partial [Bos taurus]	0.006	x	x		

Table 7: Identified proteins with positive GRAVY scores > 0

4 Discussion

4.1 Technical solution: Serial IPG gels – "Daisy Chain" gels

Modern proteomics research integrates a wide variety of analytical technologies, like two dimensional gel electrophoresis (Schrattenholz and Groebe, 2007), liquid chromatography (Godin et al., 2007), mass spectrometry (Cox and Mann, 2007), chip-based array technologies (Reid et al., 2007) and computational and mathematical concepts for bioinformatics (Adachi et al., 2007). The development, in particular in the field now called systems biology is breathtaking.

As has become apparent over the last years, resolution and accurate differential quantification, with subsequent statistical analysis of data is key to reliable surrogate biomarkers. Due to the given complexity, dynamics and stochasticity of protein expression, ever new and individual experimental strategies have to be defined for every biological sample. As has been shown by this work, the major analytical problems in proteomics is dynamic expression range or protein abundances (Corthals et al., 2000) which can be overcome by either increasing resolution (Poznanovic et al., 2005a; Neubauer et al., 2006) or prefractionation, e.g. by laser capture microdissection (Neubauer et al., 2006) to enrich relevant low abundant proteins. Also organelle fractionation and subsequent appropriate choice of separation methods (e.g. for mitochondrial membrane proteins) is a way of addressing biological questions (Hunzinger et al., 2006). The joint consideration of sample fractionation, resolution of separation and quantitative detection has led to pooling strategies which successfully identified novel protein biomarkers in cancer and ageing research (Poznanovic et al., 2005b; Neubauer et al., 2006; Groebe et al., 2007).

One prerequisite for achieving these goals was the technical development, of an easy and readily available high resolution IEF (Poznanovic et al., 2005a), which helped to improve significantly the poor separation capacity of conventional methods or the technical diffculties of high resolution approaches existing so far (Vuong et al., 2000), which needed a considerable degree of expertise and training. On the basis of this development we were able to obtain differential biomarker information working with extremely limited amounts of samples from

clinical biopsies (Neubauer et al., 2006) or cellular sub-fractions (Hunzinger et al., 2006).

In particular, the more versatile, easy and reproducible alternative to previous methods (Poland et al., 2003). using commercially available IPGs of appropriate pH ranges, in a set-up (end-on-end), which we termed "daisy chain" IEFs. (Poznanovic et al., 2005a) has meanwhile lead to a series of publications (Hunzinger et al., 2006; Groebe et al., 2007; Poznanovic et al., 2005b; Neubauer et al., 2006).

The work included the construction of a new running chamber adapted for daisy chain IEF as well as a cooling device and the optimization of a variety of parameters, like running condition, application of sample and different bridging materials, including paper, polyacrylamide gels, agarose or even IPG strips themselves. Our best results we obtained using paper and acrylamide bridges, which became routine in our lab.

Using "daisy chain" IEF high resolution in protein separation in combination with ProteoTope with the inherent sensitivity of differential and quantitative radioactive measurements provides a superior and reliable strategy for pattern control and the discovery of valid surrogate biomarkers even from very low amounts of initial sample.

4.2 Differential Radioactive Proteomic Analysis of Microdissected Renal Cell Carcinoma

Microdissected clinical samples are always extremely valuable, and therefore every experimental effort to extract an optimum of molecular information is justified. As shown here, 2D-PAGE provides the best resolution of protein species, and remains the most powerful tool available, in particular in the case of complex samples (Gorg et al., 2004; Poznanovic et al., 2005b). Optimal results are obtained by 2D-PAGE using high resolution, narrow pH gradient 'zoom gels', even more so, if assembled according to the 54 cm IEF strategy outlined in this work, which we showed to be specially suitable in the case of extremely limited sample amounts, at the same time providing the prerequisite for differential quantification of protein biomarkers (Wozny et al., 2007; Poznanovic et al., 2005b; Koellermann et al., 2008).

From two microdisected samples containing approximately 3.8 µg of protein each, after ProteoTope measurement we received reproducible 2D-PAGE patterns across inverse replicates and duplicates (Figure 12). The quality of multiplex differential quantification was excellent, achieving highly significant results (Figure 14). The analytical ProteoTope images from microdissected samples were slightly less complex than silver stained images from comparative sources (Figure 13). This effect is optically exaggerated by the poor linear dynamic range of silver staining, that makes protein spots over a wide range of abundances appear similarly dark in silver stained gels. Compared to ProteoTope gels, silver stained-images appear to be more sensitive whereas in fact they are hopelessly oversaturated. In this work we showed the optimization of radioactive pattern analysis by combination with tracer-controlled silver stained gels for mass spectrometry-based protein identification. Although proteins of lower molecular weight are more likely to lack the amino acids addressed by particular protein labelling strategies, we showed that despite the loss of some proteins our strategy provides the best current compromise.

The combination of sample microdissection and ProteoTope analysis strategies provides enormous advantages concerning the quality of quantitative protein data obtained in relation to the amount of sample consumed. The linear dynamic range and the precision of multiplex protein detection in 2D-PAGE gels by ProteoTope were widely appreciated in the Proteomics community and have lead to the discovery of novel biomarkers in cancer and neurobiology (Sommer et al., 2004; Schillo et al., 2005; Wozny et al., 2007; Koellermann et al., 2008). An other advantage of high resolution and quantitative detection is the statistical treatment of differential data, which is standard in genomic and transcriptomic array studies, has recently only been introduced into the Proteomics field by approaches like the one presented here, and is and absolutely mandatory requirement for the characterization of biomarker candidates (Schrattenholz and Groebe, 2007).

Moving from technical aspects to the biological results, the nature of differentially detected proteins identified in Figure 14 merits brief mention before concluding. Associations with cancer have been reported for the most of these proteins and is easy searchable through Medline. To discuss just a few examples in some detail, muscle-type fatty acid binding protein (M-FABP), which was absent

from cancer samples (Figure 14), is also called mammary-derived growth inhibitor (MDGI) and is a known tumor suppressor in breast cancer (Nass and Davidson, 1999). Two spots were observed for peptidylprolyl isomerase A, with the more acidic being more abundant in cancer (spots 3-37 & 3-34 in Figure 13 and Figure 14 respectively). Taken together, these results suggest possible cancer-associated phosphorylation. Several spots of annexin A4 and annexin A5 were found to be more abundant in cancer tissue (spots 2-04 & 2-05 for annexin A4; 1.-03 and 1-04 for annexin A5 in Figure 13 and Figure 14. Changes in annexin family members are often associated with cancer, e.g. (Smitherman et al., 2004) and Annexin A3 is underway as a novel alternative marker for prostate cancer (Wozny et al., 2007; Koellermann et al., 2008). We found that several of proteins associated with energy and redox regulation were differential between normal and cancer cells, which was an expected result. Taken together, the identities of the differential proteins identified by ProteoTope from microdissected samples are most likely to reflect real differences in the samples of origin, validating the technique. Indeed, since the samples of origin were relatively homogeous, many of the protein differences were still apparent at the silver stained level (Figure 13), further corroborating that ProteoTope was able to accurately portray the protein profile in the microdissected experimental samples.

We showed that the method used in this work is very well suited to enable comprehensive multiplex proteomic analyses, using standard 2 µm clinical biopsies, which are standard in a routine practice in many clinics.

4.3 Breast cancer proteomics by laser capture micro dissection

Some of the previous studies with laser microdissection samples had a tendency to analyze multiple patient samples combined into one large pools (Wulfkuhle et al., 2002), or have provided isolated proof-of-principle examples from single or few patients using saturation labeling on lysine with fluorescent Cy dyes in combination with two-dimensional difference gel electrophoresis (2D-DIGE) (Sitek et al., 2005; Greengauz-Roberts et al., 2005; Kondo et al., 2003). The former class of studies is vulnerable to atypical abundant signals from single patients. The latter class of study lacks the element of systematic population sampling and associated stringent statistical analysis to exclude those proteins whose abundances vary due to inter-individual differences that are not correlated

with experimental test variables. Indeed, not all studies demonstrated that the obtained 2D-PAGE patterns would be reproducible in duplicate experiments, while others suggested that this might in fact be problematical.

In an innovative recent strategic development, Cy dye 2D-DIGE was used to profile 30 lung cancer cell lines of different histological types (Seike et al., 2005). Cluster analysis revealed 32 spots from cultured cell lines that correlated with histological type of the parent tumors, of which 14 spots could be identified. They then analyzed micro dissected tissue samples, using an area of 1 mm2 of micro dissected cancer tissue from 10 µm thick cryosections for each gel, which corresponds to approximately 0.5 µg of protein (± ≈ 20%). Cancerous cells from 30 tumors were examined by LCM and 2D-DIGE. Based on the multivariate analysis of the DIGE intensities of the same 32 spots already detected from cell cultured lines, the tumors clustered in a hierarchical tree whose structure closely reflected the prior information on the histology of origin of their parental tumors. While this experimental strategy is impressive, it contains an implicit assumption that the statistical characterization of the 32 key spots detected from cell cultured samples could not have been identified by direct 2D-DIGE analysis of microdissected cancer samples. It was uncertain from the above publication whether this is true, yet, pursuing the associated implications, the strategy would be dependent upon obtaining similar protein expression of marker proteins in cell lines and tissues. This would in turn impose an undesirable restriction of the method to an uncertain subset of clinical applications, because cell lines are well known to typically deviate from the gene expression profiles of their progenitor cells.

As we showed in this work using our approach we were able to detect and identify proteins that were significantly differential between two clinically well-defined populations of micro dissected primary tumors, using very well characterized clinical samples for which no suitable cell line models exist. Regarding the quality of results, it can be noted particularly that ER+/PR- tumors consistently exhibited just 1.5-fold higher levels of SPUF/neudesin, however ProteoTope was able to quantify this differential ratio with precision and sensitivity sufficient to generate a t-test probability of 0.002. To my knowledge, a comparable result has not previously been achieved using 2D-DIGE. This shows that ProteoTope with his higher dynamic range than DIGE and in combination with high resolution IEF-

2D-PAGE is a very useful method especially in cases when only small or even minute amounts of material are available.

Relatively few proteins exhibited significant differential abundance between all tested pools from each test population (Figure 17, Figure 18), demonstrating that sample pooling was not disadvantageous, but rather delivered a modest number of differential proteins, of which several evaded identification by mass spectrometry. Many significant proteins were previously unreported in relation to PR status, or even to breast cancer. Overall, relative to the more aggressive ER+/PR- tumors, ER+/PR+ samples exhibited higher levels of immunoglobulin kappa light chain, and lower cathepsin D and hemoglobin levels. Both estrogen and progesterone are thought to affect breast cells by inducing the production of paracrine factors by ER- and/or PR-containing cells. These factors are then thought to induce the cellular proliferation of neighboring cells that lack steroid receptors (Anderson and Clarke, 2004). Therefore it is highly relevant to consider possible paracrine associations for the differential identified proteins. Notably, from the 7 proteins that exhibited significances of $p < 0.01$ in Figure 18, cellular retinoic acid binding protein type II (CRABP-II) features along with both microsomal cytochrome b5 (Cyt-b5) and Neudesin/SPUF (Neubauer et al., 2006).

Retinoids, natural and synthetic derivatives of vitamin A, mediate antiproliferative and proapoptotic effects by inducing differentiation and/or growth arrest, was making them a promising class of chemopreventive agents against breast cancer. They bind to homo- or heterodimers of the retinoic acid (RAR) or retinoid X (RXR) receptor families, as well as other proteins, and the concentrations of these components influence the retinoid response (Simeone and Tari, 2004; Niles, 2004). Higher levels of the RAR-alpha are associated with greater proliferation rates of ER-positive ductal carcinoma in situ (Ariga et al., 2000). Retinoid receptors influence a diverse range of proteins involved in signal transduction and cell cycle control, and make direct protein interaction with various kinases and transcription factors (Niles, 2004). From this perspective, possible effects of elevated amounts of CRABP-II in ER+/PR- tumors could include binding and sequestering intracellular retinoic acid to reduce the general availability to retinoid receptors, to preferentially deliver retinoic acid to particular receptors, or to channel it preferentially into specific metabolic pathways and so affect its cellular availability (Niles, 2004). This could thereby reduce the antiproliferative and

proapoptotic effects of retinoids on cancer growth, and potentiate clinical malignacy.

Both Neudesin/SPUF and Cyt-b5 are cytochrome b5 domain-containing proteins. Cyt-b5 is a recognized erythrocyte constituent, yet is less abundant in ER+/PR- tumors, whereas hemoglobin is more abundant in those tissues (Figure 18), therefore Cyt-b5 apparently exhibits higher levels in ER+/PR- tissue independently of the presence of erythrocytes. Neudesin/SPUF, was recently identified as a secreted neural protein with neurotrophic activity, acting through a pertussis toxin-sensitive Gi/G0-protein-coupled receptor (Simeone and Tari, 2004). There is a possibility that both, Cyt-b5 and SPUF/neudesin could conceivably be involved in binding signaling molecules, such as progestins, that might mediate cancer-relevant signaling functions. This point was pursued because Hpr6.6 (also called "membrane associated progesterone receptor component 1") binds to progesterone via a related cytochrome b5 domain (Mifsud and Bateman, 2002). The potential relevance hereof is that at least the Hpr6.6 cytochrome b5 domain does bind progesterone, and the experimental test variable under consideration in the present study was none other than the presence or absence of a receptor for this ligand.

Cyt-b5, a heme-binding protein, is classically involved in the introduction of double bonds into long-chain acyl Coenzyme A molecules to generate unsaturated fatty acids, and positively regulates some reactions catalyzed by cytochrome P450 proteins (P450s) expressed in breast tissue (Schenkman and Jansson, 2003; Lamb et al., 1999). The Cyt-b5 related Dap1p proteins are proposed to activate the cytochrome P450 protein Cyp21, elevating the oxidation of progesterone in the liver (Min et al., 2004). The yeast Dap1p cytochrome b5 domain protein indeed regulates P450 activity and affects sterol synthesis (Mallory et al., 2005). Cyt-b5 allosterically regulates the activity of P450 17 (independent of hemebinding) to favour the production of sex steroids rather than glucocorticoids from the metabolism of progesterone (Porter, 2002). Thus, Cyt-b5 could affect P450 protein regulated mechanisms, such as the in situ aromatization of steroid hormones; and metabolism and detoxification of drugs and xenobiotic agents (Brock and Waterman, 1999; Williams and Phillips, 2000; Nebert and Russell, 2002). Because regulating the concentration of progesterone is recognised to be important in controling its autocrine or paracrine effects on tumor growth

(Anderson and Clarke, 2004), modulations of hormone concentration at a subcellular level are conceivable, as proposed above, and could effect the function of Cyt-b5.

Taken together, and as discussed previously (Neubauer et al., 2006), these results suggest that altered intratumoral expression of genes coding for xenobiotic-metabolizing enzymes might be responsible for different susceptibility of ER^+/PR^+ and ER^+/PR^- tumors against tamoxifen. Currently, PR is a surrogate marker of estrogen receptor activity that is used to predict clinical outcome, most recently as assayed by immunehistochemistry (Mohsin et al., 2004). The results of Figure 18 indicate that the abundance of Cyt-b5 (higher abundance associated with significantly improved disease-free and overall survival -ER^+/PR^-) and CRABP-II (lower abundance associated with significantly improved disease-free and overall survival – ER^+/PR^+) may offer additional useful diagnostic parameters to improve choice of clinical therapy. Irrespective thereof, SPUF/neudesin and/or CRABP-II might thus differentially modulate the biology of tumors of differing progesterone receptor status, and may represent candidate drug targets for the treatment of breast cancer cells that lack the PR.

4.4 Comparative Profiling of the Mammalian Mitochondrial Proteome

Estimations show that number of proteins in mammalian mitochondria should vary between 1500-4000 (Taylor et al., 2003b; Heazlewood et al., 2003; Calvo et al., 2006) but only 680 proteins have been found so far (Taylor et al., 2003b; Calvo et al., 2006). As shown Table 4 from our IEF/2D PAGE experiment we detected 1008 spots and 745 spots were picked, digested and submitted to the MALDI-TOF peptide mass fingerprint analysis. We identified 400 proteins and among them 123 nonredundant proteins. In contrast to this result we detected 172 proteins in blue native experiment and 71 were identified as nonredundant. In 16-BAC experiment we detected 121 proteins and identified 30 nonredundant ones and in tricine-urea experiment we detected 117 proteins and identified 41 nonredundant ones.

Main aim of this work wasn't to make any inventory of mitochondrial proteins but to benchmark the best analytical methods for ROS- and age-related changes of mitochondrial proteins. We wanted to define an experimental window

likely to reflect a maximum of information about corresponding posttranslational modifications in relevant proteins at an optimal results/cost ratio. Whole work was done as exploratory study for a European 6th Framework Project (www.mimage.org). Therefore not only resolution was considered, and thus applicability to quantitative differential display and statistical analysis of a method, but also the bias towards detecting certain types of proteins had to be examined and quantified. In a non-comprehensive fashion, and a in selected experimental window, the comparison of four 2D PAGE methods showed the superiority of 2D IEF-SDS-PAGE over all other methods in terms of resolution. (Hunzinger et al., 2006) This finding is not surprising, but implies (because the same uniform preparation of bovine heart mitochondria was used in all experiments) that the other methods are hardly applicable for a differential gel-based study, especially if isotopic labeling of the samples is considered (because always multiple non-resolved protein locations species in a single position would obscure isoform assignments and their quantifications by isotopic labeling, a problem of each and every method associated with lower resolution methods, including most LC-MS approaches) (Schrattenholz, 2004; Zolg and Langen, 2004).

Beyond resolution, the biological relation of the proteins identified to ROS- and age-related processes and mitochondrial or intrinsic apoptotic mechanisms was of interest for this work (Eldadah and Faden, 2000; Saraste and Pulkki, 2000). On a first level, hydrophobic integral membrane proteins appear to be relevant in a variety of studies concerning mitochondrial proteomes, and GRAVY scores are recently used frequently to address the coverage of these proteins by various proteomic methods (Blonder et al., 2004; Jiang et al., 2004). Under given conditions, without prior pre-fractionations in order to obtain sufficient coverage of imported/exported proteins, potentially signaling age-related ROS-effects to the cytosol, (especially components of the intrinsic or mitochondrial apoptotic pathway), essentially only 2D IEF/SDS-PAGE was able to resolve mitochondrial permeability transition pore (MPTP) proteins like e.g. ANT-1, whereas the AIF appeared exclusively in the 16-BAC method.

Recently, it has been found, that some mitochondrial citric acid cycle enzymes are altered during the normal aging process. This is true for both NADP+ dependent isocitrate dehydrogenase (IDPm) (Kil et al., 2004b), which was found in several isoforms in this work, but and in particular, for aconitase-2, which has

been implicated as playing a key role as an age-related marker in a variety of organisms and organs (Shadel, 2005; Delaval et al., 2004; Liang and Patel, 2004). In flight muscle mitochondria of houseflies of different ages, aconitase was the only enzyme that exhibiting exhibited altered activity during aging (Yarian and Sohal, 2005). It has moreover been suggested that aging induced post-translational oxidative modifications occur during the aging process and thus results in functional alterations. Adducts with malondialdehyde (MDA), a product of lipid peroxidation, were among those found for aconitase, very long chain acyl coenzyme A dehydrogenase, ATP synthase and alpha-ketoglutarate dehydrogenase (Liang and Patel, 2004). The decreasing activities of these proteins have also been implicated as well in progress of aging-related processes. These proteins were all identified in this work, indeed MDA adducts was observed. The ferric ion of aconitase is moreover a target of signaling via nitric oxide NO and its metabolites peroxynitrite and the nitroxyl anion (Castro et al., 1994; Cooper, 1999; Gardner et al., 1997).

Since mitochondria are both a major source of oxidants and a target for their damaging effects, and since mitochondrial oxidative stress appears to be the major cause of cell aging, and since this type of oxidative damage in aging is particularly high in mitochondrial DNA and aconitase, special attention was rather paid to the isoform pattern of this enzyme, and moreover to components of the related intrinsic apoptotic pathway. In the follow-up the approach has been successfully been applied to differentially profile age-elated changes in Podospora, human and rodent mitochondria (Groebe et al., 2007) and very recently in material from Drosophila and Caenorhabditis (yet unpublished).

5 Conclusion

Biomarkers play an important role in molecular medicine. Proteomics has been recognized as key to biomarkers discovery, based on the assumption that disease-related processes alter the protein signatures of complex biological systems. The differential quantitative analysis of protein expression profiles with the aim of discovering surrogate biomarkers is currently fuelling the technical development in separation technologies, mass spectrometry and bioinformatics.

Here we show that high resolution 2D-PAGE in combination with isotopic labeling is one of the best compromises currently available. This work is about the development of a new and convenient method for high resolution IEF of proteins which we termed: "daisy chain" (Poznanovic et al., 2005a). This method was subsequently successfully applied to valuable clinical samples from cancer patients (Neubauer et al., 2006; Poznanovic et al., 2005b; Wozny et al., 2007) and to mitochondrial preparations related to a European project in gerontology (Groebe et al., 2007). We thus developed a suite of experimental strategies which adequately address complex biological situations, in particular on the level of protein expression. As shown in selected cases by subsequent independent validation, the essential prerequisite for a reliable biomarker characterization is the statistical treatment of differential quantities in relevant biological material (Koellermann et al., 2008; Schrattenholz and Groebe, 2007; Schostak et al., 2008).

6 Bibliography

Adachi,J., Kumar,C., Zhang,Y. and Mann,M. (2007) In-depth analysis of the adipocyte proteome by mass spectrometry and bioinformatics. Mol. Cell Proteomics., 6, 1257-1273.

Anderson,E. and Clarke,R.B. (2004) Steroid receptors and cell cycle in normal mammary epithelium. J. Mammary. Gland. Biol. Neoplasia., 9, 3-13.

Ariga,N., Moriya,T., Suzuki,T., Kimura,M., Ohuchi,N. and Sasano,H. (2000) Retinoic acid receptor and retinoid X receptor in ductal carcinoma in situ and intraductal proliferative lesions of the human breast. Jpn. J. Cancer Res., 91, 1169-1176.

Beadle,G.W. and Tatum,E.L. (1941) Genetic Control of Biochemical Reactions in Neurospora. Proc. Natl. Acad. Sci. U. S. A., 27, 499-506.

Blonder,J., Goshe,M.B., Xiao,W., Camp,D.G., Wingerd,M., Davis,R.W. and Smith,R.D. (2004) Global analysis of the membrane subproteome of Pseudomonas aeruginosa using liquid chromatography-tandem mass spectrometry. J. Proteome. Res., 3, 434-444.

Brock,B.J. and Waterman,M.R. (1999) Biochemical differences between rat and human cytochrome P450c17 support the different steroidogenic needs of these two species. Biochemistry, 38, 1598-1606.

Brookes,P.S., Pinner,A., Ramachandran,A., Coward,L., Barnes,S., Kim,H. and Darley-Usmar,V.M. (2002) High throughput two-dimensional blue-native electrophoresis: a tool for functional proteomics of mitochondria and signaling complexes. Proteomics., 2, 969-977.

Bulteau,A.L., Lundberg,K.C., Ikeda-Saito,M., Isaya,G. and Szweda,L.I. (2005) Reversible redox-dependent modulation of mitochondrial aconitase and proteolytic activity during in vivo cardiac ischemia/reperfusion. Proc. Natl. Acad. Sci. U. S. A, 102, 5987-5991.

Butcher,E.C. (2005) Can cell systems biology rescue drug discovery? Nat. Rev. Drug Discov., 4, 461-467.

Cahill,M.A., Wozny,W., Schwall,G., Schroer,K., Holzer,K., Poznanovic,S., Hunzinger,C., Vogt,J.A., Stegmann,W., Matthies,H. and Schrattenholz,A. (2003) Analysis of relative isotopologue abundances for quantitative profiling of complex protein mixtures labelled with the acrylamide/D3-acrylamide alkylation tag system. Rapid Commun. Mass Spectrom., 17, 1283-1290.

Calvo,S., Jain,M., Xie,X., Sheth,S.A., Chang,B., Goldberger,O.A., Spinazzola,A., Zeviani,M., Carr,S.A. and Mootha,V.K. (2006) Systematic identification of human mitochondrial disease genes through integrative genomics. Nat. Genet., 38, 576-582.

Castro,L., Rodriguez,M. and Radi,R. (1994) Aconitase is readily inactivated by peroxynitrite, but not by its precursor, nitric oxide. J. Biol. Chem., 269, 29409-29415.

Chen,X.J., Wang,X., Kaufman,B.A. and Butow,R.A. (2005) Aconitase couples metabolic regulation to mitochondrial DNA maintenance. Science, 307, 714-717.

Cooper,C.E. (1999) Nitric oxide and iron proteins. Biochim. Biophys. Acta, 1411, 290-309.

Corthals,G.L., Wasinger,V.C., Hochstrasser,D.F. and Sanchez,J.C. (2000) The dynamic range of protein expression: a challenge for proteomic research. Electrophoresis., 21, 1104-1115.

Cox,J. and Mann,M. (2007) Is proteomics the new genomics? Cell., 130, 395-398.

Delaval,E., Perichon,M. and Friguet,B. (2004) Age-related impairment of mitochondrial matrix aconitase and ATP-stimulated protease in rat liver and heart. Eur. J. Biochem., 271, 4559-4564.

Devreese,B., Vanrobaeys,F., Smet,J., Van Beeumen,J. and Van Coster,R. (2002) Mass spectrometric identification of mitochondrial oxidative phosphorylation subunits separated by two-dimensional blue-native polyacrylamide gel electrophoresis. Electrophoresis, 23, 2525-2533.

Duncan,M.W. and Hunsucker,S.W. (2005) Proteomics as a tool for clinically relevant biomarker discovery and validation. Exp. Biol. Med. (Maywood.)., 230, 808-817.

Edman,P. and Begg,G. (1967) A protein sequenator. Eur. J. Biochem., 1, 80-91.

Eldadah,B.A. and Faden,A.I. (2000) Caspase pathways, neuronal apoptosis, and CNS injury. J. Neurotrauma, 17, 811-829.

Emmert-Buck,M.R., Bonner,R.F., Smith,P.D., Chuaqui,R.F., Zhuang,Z., Goldstein,S.R., Weiss,R.A. and Liotta,L.A. (1996) Laser capture microdissection. Science., 274, 998-1001.

Etzioni,R., Urban,N., Ramsey,S., McIntosh,M., Schwartz,S., Reid,B., Radich,J., Anderson,G. and Hartwell,L. (2003) The case for early detection. Nat. Rev. Cancer., 3, 243-252.

Forner,F., Foster,L.J., Campanaro,S., Valle,G. and Mann,M. (2006) Quantitative proteomic comparison of rat mitochondria from muscle, heart, and liver. Mol. Cell Proteomics., 5, 608-619.

Franzen,B., Hirano,T., Okuzawa,K., Uryu,K., Alaiya,A.A., Linder,S. and Auer,G. (1995) Sample preparation of human tumors prior to two-dimensional electrophoresis of proteins. Electrophoresis., 16, 1087-1089.

Fujii,K., Nakano,T., Kawamura,T., Usui,F., Bando,Y., Wang,R. and Nishimura,T. (2004) Multidimensional protein profiling technology and its application to human plasma proteome. J. Proteome. Res., 3, 712-718.

Gardner,P.R., Costantino,G., Szabo,C. and Salzman,A.L. (1997) Nitric oxide sensitivity of the aconitases. J. Biol. Chem., 272, 25071-25076.

Gingras,A.C., Gstaiger,M., Raught,B. and Aebersold,R. (2007) Analysis of protein complexes using mass spectrometry. Nat. Rev. Mol. Cell Biol., 8, 645-654.

Godin,J.P., Fay,L.B. and Hopfgartner,G. (2007) Liquid chromatography combined with mass spectrometry for 13C isotopic analysis in life science research. Mass Spectrom. Rev., 26, 751-774.

Gorg,A., Weiss,W. and Dunn,M.J. (2004) Current two-dimensional electrophoresis technology for proteomics. Proteomics., 4, 3665-3685.

Greengauz-Roberts,O., Stoppler,H., Nomura,S., Yamaguchi,H., Goldenring,J.R., Podolsky,R.H., Lee,J.R. and Dynan,W.S. (2005) Saturation labeling with cysteine-reactive cyanine fluorescent dyes provides increased sensitivity for protein expression profiling of laser-microdissected clinical specimens. Proteomics., 5, 1746-1757.

Groebe,K., Krause,F., Kunstmann,B., Unterluggauer,H., Reifschneider,N.H., Scheckhuber,C.Q., Sastri,C., Stegmann,W., Wozny,W., Schwall,G.P., Poznanovic,S., Dencher,N.A., Jansen-Durr,P., Osiewacz,H.D. and Schrattenholz,A. (2007) Differential proteomic profiling of mitochondria from Podospora anserina, rat and human reveals distinct patterns of age-related oxidative changes. Exp. Gerontol., 42, 887-898.

Hanahan,D. and Weinberg,R.A. (2000) The hallmarks of cancer. Cell., 100, 57-70.

Harry,J.L., Wilkins,M.R., Herbert,B.R., Packer,N.H., Gooley,A.A. and Williams,K.L. (2000) Proteomics: capacity versus utility. Electrophoresis., 21, 1071-1081.

Hartinger,J., Stenius,K., Hogemann,D. and Jahn,R. (1996) 16-BAC/SDS-PAGE: a two-dimensional gel electrophoresis system suitable for the separation of integral membrane proteins. Anal. Biochem., 240, 126-133.

Heazlewood,J.L., Millar,A.H., Day,D.A. and Whelan,J. (2003) What makes a mitochondrion? Genome Biol., 4, 218.

Henzel,W.J., Billeci,T.M., Stults,J.T., Wong,S.C., Grimley,C. and Watanabe,C. (1993) Identifying proteins from two-dimensional gels by molecular mass searching of peptide fragments in protein sequence databases. Proc. Natl. Acad. Sci. U. S. A., 90, 5011-5015.

Huang,H.L., Stasyk,T., Morandell,S., Dieplinger,H., Falkensammer,G., Griesmacher,A., Mogg,M., Schreiber,M., Feuerstein,I., Huck,C.W., Stecher,G., Bonn,G.K. and Huber,L.A. (2006) Biomarker discovery in breast cancer serum using 2-D differential gel electrophoresis/ MALDI-TOF/TOF and data validation by routine clinical assays. Electrophoresis., 27, 1641-1650.

Hunzinger,C., Wozny,W., Schwall,G.P., Poznanovic,S., Stegmann,W., Zengerling,H., Schoepf,R., Groebe,K., Cahill,M.A., Osiewacz,H.D., Jagemann,N., Bloch,M., Dencher,N.A., Krause,F. and Schrattenholz,A. (2006) Comparative profiling of the mammalian mitochondrial proteome: multiple aconitase-2 isoforms including N-formylkynurenine modifications as part of a protein biomarker signature for reactive oxidative species. J. Proteome. Res., 5, 625-633.

Issaq,H.J. and Veenstra,T.D. (2007) The role of electrophoresis in disease biomarker discovery. Electrophoresis., 28, 1980-1988.

Jiang,X.S., Zhou,H., Zhang,L., Sheng,Q.H., Li,S.J., Li,L., Hao,P., Li,Y.X., Xia,Q.C., Wu,J.R. and Zeng,R. (2004) A high-throughput approach for subcellular proteome: identification of rat liver proteins using subcellular fractionation coupled with two-dimensional liquid chromatography tandem mass spectrometry and bioinformatic analysis. Mol. Cell Proteomics., 3, 441-455.

Jo,S.H., Son,M.K., Koh,H.J., Lee,S.M., Song,I.H., Kim,Y.O., Lee,Y.S., Jeong,K.S., Kim,W.B., Park,J.W., Song,B.J. and Huh,T.L. (2001) Control of mitochondrial redox balance and cellular defense against oxidative damage by mitochondrial NADP+-dependent isocitrate dehydrogenase. J. Biol. Chem., 276, 16168-16176.

Kil,I.S., Lee,J.H., Shin,A.H. and Park,J.W. (2004a) Glycation-induced inactivation of NADP(+)-dependent isocitrate dehydrogenase: implications for diabetes and aging. Free Radic. Biol. Med., 37, 1765-1778.

Kil,I.S., Lee,Y.S., Bae,Y.S., Huh,T.L. and Park,J.W. (2004b) Modulation of NADP(+)-dependent isocitrate dehydrogenase in aging. Redox. Rep., 9, 271-277.

Kil,I.S. and Park,J.W. (2005) Regulation of mitochondrial NADP+-dependent isocitrate dehydrogenase activity by glutathionylation. J. Biol. Chem., 280, 10846-10854.

Koellermann,J., Schlomm,T., Bang,H., Schwall,G.P., Eichel-Streiber,C., Simon,R., Schostak,M., Huland,H., Berg,W., Sauter,G., Klocker,H. and Schrattenholz,A. (2008) Expression and Prognostic Relevance of Annexin A3 in Prostate Cancer.

Kondo,T., Seike,M., Mori,Y., Fujii,K., Yamada,T. and Hirohashi,S. (2003) Application of sensitive fluorescent dyes in linkage of laser microdissection and two-dimensional gel electrophoresis as a cancer proteomic study tool. Proteomics., 3, 1758-1766.

Krause,F., Reifschneider,N.H., Goto,S. and Dencher,N.A. (2005) Active oligomeric ATP synthases in mammalian mitochondria. Biochem. Biophys. Res. Commun., 329, 583-590.

Krause,F., Scheckhuber,C.Q., Werner,A., Rexroth,S., Reifschneider,N.H., Dencher,N.A. and Osiewacz,H.D. (2004) Supramolecular organization of cytochrome c oxidase- and alternative oxidase-dependent respiratory chains in the filamentous fungus Podospora anserina. J. Biol. Chem., 279, 26453-26461.

Kyte,J. and Doolittle,R.F. (1982) A simple method for displaying the hydropathic character of a protein. J. Mol. Biol., 157, 105-132.

Lamb,D.C., Kelly,D.E., Manning,N.J., Kaderbhai,M.A. and Kelly,S.L. (1999) Biodiversity of the P450 catalytic cycle: yeast cytochrome b5/NADH cytochrome b5 reductase complex efficiently drives the entire sterol 14-demethylation (CYP51) reaction. FEBS Lett., 462, 283-288.

Liang,L.P. and Patel,M. (2004) Iron-sulfur enzyme mediated mitochondrial superoxide toxicity in experimental Parkinson's disease. J. Neurochem., 90, 1076-1084.

Liotta,L.A. and Kohn,E.C. (2001) The microenvironment of the tumour-host interface. Nature., 411, 375-379.

Mallory,J.C., Crudden,G., Johnson,B.L., Mo,C., Pierson,C.A., Bard,M. and Craven,R.J. (2005) Dap1p, a heme-binding protein that regulates the cytochrome P450 protein Erg11p/Cyp51p in Saccharomyces cerevisiae. Mol. Cell Biol., 25, 1669-1679.

Mann,M. (2006) Functional and quantitative proteomics using SILAC. Nat. Rev. Mol. Cell Biol., 7, 952-958.

Marko-Varga,G., Lindberg,H., Lofdahl,C.G., Jonsson,P., Hansson,L., Dahlback,M., Lindquist,E., Johansson,L., Foster,M. and Fehniger,T.E. (2005) Discovery of biomarker candidates within disease by protein profiling: principles and concepts. J. Proteome. Res. , 4, 1200-1212.

Mifsud,W. and Bateman,A. (2002) Membrane-bound progesterone receptors contain a cytochrome b5-like ligand-binding domain. Genome Biol., 3, RESEARCH0068.

Min,L., Takemori,H., Nonaka,Y., Katoh,Y., Doi,J., Horike,N., Osamu,H., Raza,F.S., Vinson,G.P. and Okamoto,M. (2004) Characterization of the adrenal-specific antigen IZA (inner zone antigen) and its role in the steroidogenesis. Mol. Cell Endocrinol., 215, 143-148.

Mohsin,S.K., Weiss,H., Havighurst,T., Clark,G.M., Berardo,M., Roanh,l.D., To,T.V., Qian,Z., Love,R.R. and Allred,D.C. (2004) Progesterone receptor by immunohistochemistry and clinical outcome in breast cancer: a validation study. Mod. Pathol., 17, 1545-1554.

Nass,S.J. and Davidson,N.E. (1999) The biology of breast cancer. Hematol. Oncol. Clin. North Am. , 13, 311-332.

Nebert,D.W. and Russell,D.W. (2002) Clinical importance of the cytochromes P450. Lancet, 360, 1155-1162.

Neubauer,H., Clare,S.E., Kurek,R., Fehm,T., Wallwiener,D., Sotlar,K., Nordheim,A., Wozny,W., Schwall,G.P., Poznanovic,S., Sastri,C., Hunzinger,C., Stegmann,W., Schrattenholz,A. and Cahill,M.A. (2006) Breast cancer proteomics by laser capture microdissection, sample pooling, 54-cm IPG IEF, and differential iodine radioisotope detection. Electrophoresis, 27, 1840-1852.

Niles,R.M. (2004) Signaling pathways in retinoid chemoprevention and treatment of cancer. Mutat. Res., 555, 81-96.

Okuzawa,K., Franzen,B., Lindholm,J., Linder,S., Hirano,T., Bergman,T., Ebihara,Y., Kato,H. and Auer,G. (1994) Characterization of gene expression in clinical lung cancer materials by two-dimensional polyacrylamide gel electrophoresis. Electrophoresis., 15, 382-390.

Ong,S.E. and Mann,M. (2007) Stable isotope labeling by amino acids in cell culture for quantitative proteomics . Methods Mol. Biol., 359:37-52., 37-52.

Poland,J., Cahill,M.A. and Sinha,P. (2003) Isoelectric focusing in long immobilized pH gradient gels to improve protein separation in proteomic analysis. Electrophoresis, 24, 1271-1275.

Porter,T.D. (2002) The roles of cytochrome b5 in cytochrome P450 reactions. J. Biochem. Mol. Toxicol., 16, 311-316.

Poznanovic,S., Schwall,G., Zengerling,H. and Cahill,M.A. (2005a) Isoelectric focusing in serial immobilized pH gradient gels to improve protein separation in proteomic analysis. Electrophoresis, 26, 3185-3190.

Poznanovic,S., Wozny,W., Schwall,G.P., Sastri,C., Hunzinger,C., Stegmann,W., Schrattenholz,A., Buchner,A., Gangnus,R., Burgemeister,R. and Cahill,M.A. (2005b) Differential radioactive proteomic analysis of microdissected renal cell carcinoma tissue by 54 cm isoelectric focusing in serial immobilized pH gradient gels. J. Proteome. Res. , 4, 2117-2125.

Radford,D.M., Fair,K., Thompson,A.M., Ritter,J.H., Holt,M., Steinbrueck,T., Wallace,M., Wells,S.A., Jr. and Donis-Keller,H.R. (1993) Allelic loss on a chromosome 17 in ductal carcinoma in situ of the breast. Cancer Res., 53, 2947-2949.

Rais,I., Karas,M. and Schagger,H. (2004) Two-dimensional electrophoresis for the isolation of integral membrane proteins and mass spectrometric identification. Proteomics., 4, 2567-2571.

Rajasethupathy,P., Vayttaden,S.J. and Bhalla,U.S. (2005) Systems modeling: a pathway to drug discovery. Curr. Opin. Chem. Biol., 9, 400-406.

Rasmussen,R.K., Ji,H., Eddes,J.S., Moritz,R.L., Reid,G.E., Simpson,R.J. and Dorow,D.S. (1997) Two-dimensional electrophoretic analysis of human breast carcinoma proteins: mapping of proteins that bind to the SH3 domain of mixed lineage kinase MLK2. Electrophoresis., 18, 588-598.

Reid,J.D., Parker,C.E. and Borchers,C.H. (2007) Protein arrays for biomarker discovery. Curr. Opin. Mol. Ther., 9, 216-221.

Reis,E.M., Ojopi,E.P., Alberto,F.L., Rahal,P., Tsukumo,F., Mancini,U.M., Guimaraes,G.S., Thompson,G.M., Camacho,C., Miracca,E., Carvalho,A.L., Machado,A.A., Paquola,A.C., Cerutti,J.M., da Silva,A.M., Pereira,G.G., Valentini,S.R., Nagai,M.A., Kowalski,L.P., Verjovski-Almeida,S., Tajara,E.H., Dias-Neto,E., Bengtson,M.H., Canevari,R.A., Carazzolle,M.F., Colin,C., Costa,F.F., Costa,M.C., Estecio,M.R., Esteves,L.I., Federico,M.H., Guimaraes,P.E., Hackel,C., Kimura,E.T., Leoni,S.G., Maciel,R.M., Maistro,S., Mangone,F.R., Massirer,K.B., Matsuo,S.E., Nobrega,F.G., Nobrega,M.P., Nunes,D.N., Nunes,F., Pandolfi,J.R., Pardini,M.I., Pasini,F.S., Peres,T., Rainho,C.A., dos Reis,P.P., Rodrigus-Lisoni,F.C., Rogatto,S.R., dos,S.A., dos Santos,P.C., Sogayar,M.C. and Zanelli,C.F. (2005) Large-scale transcriptome analyses reveal new genetic marker candidates of head, neck, and thyroid cancer. Cancer Res., 65, 1693-1699.

Rexroth,S., Meyer zu Tittingdorf,J.M., Krause,F., Dencher,N.A. and Seelert,H. (2003) Thylakoid membrane at altered metabolic state: challenging the forgotten realms of the proteome. Electrophoresis, 24, 2814-2823.

Saraste,A. and Pulkki,K. (2000) Morphologic and biochemical hallmarks of apoptosis. Cardiovasc. Res., 45, 528-537.

Sarto,C., Marocchi,A., Sanchez,J.C., Giannone,D., Frutiger,S., Golaz,O., Wilkins,M.R., Doro,G., Cappellano,F., Hughes,G., Hochstrasser,D.F. and Mocarelli,P. (1997) Renal cell carcinoma and normal kidney protein expression. Electrophoresis., 18, 599-604.

Schagger,H. (2001) Blue-native gels to isolate protein complexes from mitochondria. Methods Cell Biol., 65, 231-244.

Schagger,H. and Pfeiffer,K. (2000) Supercomplexes in the respiratory chains of yeast and mammalian mitochondria. EMBO J., 19, 1777-1783.

Schagger,H. and von Jagow,G. (1987) Tricine-sodium dodecyl sulfate-polyacrylamide gel electrophoresis for the separation of proteins in the range from 1 to 100 kDa. Anal. Biochem., 166, 368-379.

Schenkman,J.B. and Jansson,I. (2003) The many roles of cytochrome b5. Pharmacol. Ther., 97, 139-152.

Schillo,S., Pejovic,V., Hunzinger,C., Hansen,T., Poznanovic,S., Kriegsmann,J., Schmidt,W.J. and Schrattenholz,A. (2005) Integrative proteomics: functional and molecular characterization of a particular glutamate-related neuregulin isoform. J. Proteome. Res., 4, 900-908.

Schmidt,A. and Aebersold,R. (2006) High-accuracy proteome maps of human body fluids. Genome Biol., 7, 242.

Schostak,M., Schwall,G.P., Poznanovic,S., Groebe,K., Mueller,M., Messinger,D., Miller,K., Krause,H., Pelzer,A., Horninger,W., Klocker,H., Hennenlotter,J., Feyerabend,S., Stenzl,A. and Schrattenholz,A. (2008) Annexin A3 in urine - a highly specific non invasive marker in prostate cancer early detection.

Schrattenholz,A. (2004) Proteomics: how to control highly dynamic patterns of millions of molecules and interpret changes correctly? pp. 1-8.

Schrattenholz,A. and Groebe,K. (2007) What does it need to be a biomarker? Relationships between resolution, differential quantification and statistical validation of protein surrogate biomarkers. Electrophoresis., 28, 1970-1979.

Schrattenholz,A. and Soskic,V. (2006) NMDA receptors are not alone: dynamic regulation of NMDA receptor structure and function by neuregulins and transient cholesterol-rich membrane domains leads to disease-specific nuances of glutamate-signalling. Curr. Top. Med. Chem., 6, 663-686.

Schrattenholz,A., Wozny,W., Klemm,M., Schroer,K., Stegmann,W. and Cahill,M.A. (2005) Differential and quantitative molecular analysis of ischemia complexity reduction by isotopic labeling of proteins using a neural embryonic stem cell model. J. Neurol. Sci., 229-230, 261-267.

Seike,M., Kondo,T., Fujii,K., Okano,T., Yamada,T., Matsuno,Y., Gemma,A., Kudoh,S. and Hirohashi,S. (2005) Proteomic signatures for histological types of lung cancer. Proteomics., 5, 2939-2948.

Servais,A.C., Crommen,J. and Fillet,M. (2006) Capillary electrophoresis-mass spectrometry, an attractive tool for drug bioanalysis and biomarker discovery. Electrophoresis., 27, 2616-2629.

Shadel,G.S. (2005) Mitochondrial DNA, aconitase 'wraps' it up. Trends Biochem. Sci., 30, 294-296.

Shevchenko,A., Jensen,O.N., Podtelejnikov,A.V., Sagliocco,F., Wilm,M., Vorm,O., Mortensen,P., Shevchenko,A., Boucherie,H. and Mann,M. (1996) Linking genome and proteome by mass spectrometry: large-scale identification of yeast proteins from two dimensional gels. Proc Natl Acad Sci U S A, 93, 14440-14445.

Simeone,A.M. and Tari,A.M. (2004) How retinoids regulate breast cancer cell proliferation and apoptosis. Cell Mol. Life Sci., 61, 1475-1484.

Sitek,B., Luttges,J., Marcus,K., Kloppel,G., Schmiegel,W., Meyer,H.E., Hahn,S.A. and Stuhler,K. (2005) Application of fluorescence difference gel electrophoresis saturation labelling for the analysis of microdissected precursor lesions of pancreatic ductal adenocarcinoma. Proteomics., 5, 2665-2679.

Smith,A. (1967) Preparations, properties and conditions for assay of mitochondria: slaughterhouse material, small scale. pp. 81-86.

Smitherman,A.B., Mohler,J.L., Maygarden,S.J. and Ornstein,D.K. (2004) Expression of annexin I, II and VII proteins in androgen stimulated and recurrent prostate cancer. J. Urol., 171, 916-920.

Sommer,S., Hunzinger,C., Schillo,S., Klemm,M., Biefang-Arndt,K., Schwall,G., Putter,S., Hoelzer,K., Schroer,K., Stegmann,W. and Schrattenholz,A. (2004) Molecular analysis of homocysteic acid-induced neuronal stress. J. Proteome. Res., 3, 572-581.

Soskic,V., Groebe,K. and Schrattenholz,A. (2007) Nonenzymatic posttranslational protein modifications in ageing. Exp. Gerontol., ..

Stein,L.D. (2004) Human genome: end of the beginning. Nature., 431, 915-916.

Storkel,S., Eble,J.N., Adlakha,K., Amin,M., Blute,M.L., Bostwick,D.G., Darson,M., Delahunt,B. and Iczkowski,K. (1997) Classification of renal cell carcinoma: Workgroup No. 1. Union Internationale Contre le Cancer (UICC) and the American Joint Committee on Cancer (AJCC). Cancer., 80, 987-989.

Taylor,S.W., Fahy,E., Murray,J., Capaldi,R.A. and Ghosh,S.S. (2003a) Oxidative post-translational modification of tryptophan residues in cardiac mitochondrial proteins. J. Biol. Chem., 278, 19587-19590.

Taylor,S.W., Fahy,E., Zhang,B., Glenn,G.M., Warnock,D.E., Wiley,S., Murphy,A.N., Gaucher,S.P., Capaldi,R.A., Gibson,B.W. and Ghosh,S.S. (2003b) Characterization of the human heart mitochondrial proteome. Nat. Biotechnol., 21, 281-286.

Unlu,M., Morgan,M.E. and Minden,J.S. (1997) Difference gel electrophoresis: a single gel method for detecting changes in protein extracts. Electrophoresis., 18, 2071-2077.

Vogt,J.A., Schroer,K., Holzer,K., Hunzinger,C., Klemm,M., Biefang-Arndt,K., Schillo,S., Cahill,M.A., Schrattenholz,A., Matthies,H. and Stegmann,W. (2003) Protein abundance quantification in embryonic stem cells using incomplete metabolic labelling with 15N amino acids, matrix-assisted laser desorption/ionisation time-of-flight mass spectrometry, and analysis of relative isotopologue abundances of peptides. Rapid Commun. Mass Spectrom., 17, 1273-1282.

Vuong,G.L., Weiss,S.M., Kammer,W., Priemer,M., Vingron,M., Nordheim,A. and Cahill,M.A. (2000) Improved sensitivity proteomics by postharvest alkylation and radioactive labelling of proteins. Electrophoresis, 21, 2594-2605.

Washburn,M.P., Wolters,D. and Yates,J.R. (2001) Large-scale analysis of the yeast proteome by multidimensional protein identification technology. Nat Biotechnol, 19, 242-247.

Westermeier,R., Postel,W., Weser,J. and Gorg,A. (1983) High-resolution two-dimensional electrophoresis with isoelectric focusing in immobilized pH gradients. J. Biochem. Biophys. Methods., 8, 321-330.

Wilkins,M.R., Sanchez,J.C., Williams,K.L. and Hochstrasser,D.F. (1996) Current challenges and future applications for protein maps and post-translational vector maps in proteome projects. Electrophoresis, 17, 830-838.

Williams,J.A. and Phillips,D.H. (2000) Mammary expression of xenobiotic metabolizing enzymes and their potential role in breast cancer. Cancer Res., 60, 4667-4677.

Wirth,P.J., Egilsson,V., Gudnason,V., Ingvarsson,S. and Thorgeirsson,S.S. (1987) Specific polypeptide differences in normal versus malignant human breast tissues by two-dimensional electrophoresis. Breast Cancer Res. Treat., 10, 177-189.

Wozny,W., Schroer,K., Schwall,G.P., Poznanovic,S., Stegmann,W., Dietz,K., Rogatsch,H., Schaefer,G., Huebl,H., Klocker,H., Schrattenholz,A. and Cahill,M.A. (2007) Differential radioactive quantification of protein abundance ratios between benign and malignant prostate tissues: cancer association of annexin A3. Proteomics., 7, 313-322.

Wright,G.L., Jr. (2002) SELDI proteinchip MS: a platform for biomarker discovery and cancer diagnosis. Expert. Rev. Mol. Diagn., 2, 549-563.

Wulfkuhle,J.D., Sgroi,D.C., Krutzsch,H., McLean,K., McGarvey,K., Knowlton,M., Chen,S., Shu,H., Sahin,A., Kurek,R., Wallwiener,D., Merino,M.J., Petricoin,E.F., III, Zhao,Y. and Steeg,P.S. (2002) Proteomics of human breast ductal carcinoma in situ. Cancer Res., 62, 6740-6749.

Yang,E.S., Yang,J.H., Park,J.E. and Park,J.W. (2005) Oxalomalate, a competitive inhibitor of NADP+ -dependent isocitrate dehydrogenase, regulates lipid peroxidation-mediated apoptosis in U937 cells. Free Radic. Res., 39, 89-94.

Yarian,C.S., Rebrin,I. and Sohal,R.S. (2005) Aconitase and ATP synthase are targets of malondialdehyde modification and undergo an age-related decrease in activity in mouse heart mitochondria. Biochem. Biophys. Res. Commun., 330, 151-156.

Yarian,C.S. and Sohal,R.S. (2005) In the aging housefly aconitase is the only citric acid cycle enzyme to decline significantly. J. Bioenerg. Biomembr., 37, 91-96.

Zahedi,R.P., Meisinger,C. and Sickmann,A. (2005) Two-dimensional benzyldimethyl-n-hexadecylammonium chloride/SDS-PAGE for membrane proteomics. Proteomics., 5, 3581-3588.

Zolg,J.W. and Langen,H. (2004) How industry is approaching the search for new diagnostic markers and biomarkers. Mol. Cell Proteomics., 3, 345-354